bioRxiv preprint doi: https://doi.org/10.1101/2022.05.17.492371; this version posted May 17, 2022. The copyright holder for this preprint (which was not certified by peer review) is the author/funder, who has granted bioRxiv a license to display the preprint in perpetuity. It is made available under aCC-BY-NC 4.0 International license.

X-ray imaging of 30 year old wine grape wood reveals cumulative impacts of rootstocks on scion secondary growth and harvest index

Zoë Migicovsky[a], Michelle Y. Quigley[b], Joey Mullins[b], Tahira Ali[c,d], Joel F. Swift[e], Anita Rose Agasaveeran[f], Joseph D. Dougherty[g,h], Brendan Michael Grant[i,j], Ilayda Korkmaz[c,k], Maneesh Reddy Malpeddi[i,j], Emily L. McNichol[h,g], Andrew W. Sharp[l,g], Jackie L. Harris[m], Danielle R. Hopkins[m], Lindsay M. Jordan[m,n], Misha T. Kwasniewski[o], R. Keith Striegler[m], Asia L. Dowtin[p], Stephanie Stotts[q,r], Peter Cousins[s], Daniel H. Chitwood[b,g]

[a]Plant, Food, and Environmental Sciences, Faculty of Agriculture, Dalhousie University, Truro, Nova Scotia, B2N 5E3, Canada

[b]Department of Horticulture, Michigan State University, East Lansing, MI, 48823, USA

[c]College of Natural Science, Michigan State University, East Lansing, MI, 48823, USA

[d]Department of Neuroscience, Michigan State University, East Lansing, MI, 48823, USA

[e]Department of Biology, Saint Louis University, St. Louis, MO, 63103, USA

[f]Department of Physics and Astronomy, Michigan State University, East Lansing, MI, 48823, USA

[g]Department of Computational Mathematics, Science & Engineering, Michigan State University, East Lansing, MI, 48823, USA

[h]College of Engineering, Michigan State University, East Lansing, MI, 48823, USA

[i]College of Social Science, Michigan State University, East Lansing, MI, 48823, USA

[j]Department of Economics, Michigan State University, East Lansing, MI, 48823, USA

[k]Department of Biochemistry and Molecular Biology, Michigan State University, East Lansing, MI, 48823, USA

[l]College of Arts and Letters, Michigan State University, East Lansing, MI, 48823, USA

[m]E. & J. Gallo Winery, Acampo, CA, 95220, USA

[n]Current affiliation: Constellation Brands, Soledad, CA, USA

[o]Department of Food Science,The Pennsylvania State University

[p]Department of Forestry, Michigan State University, East Lansing, MI, 48823, USA

[q]Department of Agriculture, Food, and Resource Sciences, University of Maryland Eastern Shore, Princess Anne, MD, 21853, USA

[r]Department of Natural Sciences, University of Maryland Eastern Shore, Princess Anne, MD, 21853, USA

[s]E. & J. Gallo Winery, Modesto, CA, USA

bioRxiv preprint doi: https://doi.org/10.1101/2022.05.17.492371; this version posted May 17, 2022. The copyright holder for this preprint (which was not certified by peer review) is the author/funder, who has granted bioRxiv a license to display the preprint in perpetuity. It is made available under aCC-BY-NC 4.0 International license.

Summary

- Annual rings from 30 year old vines in a California rootstock trial were measured to determine the effects of 15 different rootstocks on Chardonnay and Cabernet Sauvignon scions. Viticultural traits measuring vegetative growth, yield, berry quality, and nutrient uptake were collected at the beginning and end of the lifetime of the vineyard.
- X-ray Computed Tomography (CT) was used to measure ring widths in 103 vines. Ring width was modeled as a function of ring number using a negative exponential model. Early and late wood ring widths, cambium width, and scion trunk radius were correlated with 27 traits.
- Modeling of annual ring width shows that scions alter the width of the first rings but that rootstocks alter the decay thereafter, consistently shortening ring width throughout the lifetime of the vine. The ratio of yield to vegetative growth, juice pH, photosynthetic assimilation and transpiration rates, and stomatal conductance are correlated with scion trunk radius.
- Rootstocks modulate secondary growth over years, altering hydraulic conductance, physiology, and agronomic traits. Rootstocks act in similar but distinct ways from climate to modulate ring width, which borrowing techniques from dendrochronology, can be used to monitor both genetic and environmental effects in woody perennial crop species.

Key words: dendrochronology, hydraulic conductance, perennial, physiology, rootstocks, viticulture, wine, wood anatomy

Introduction

Grafting is the joining of plant tissues together, through either natural or artificial means (Gaut *et al.*, 2019). When a root system (the rootstock) is grafted to a shoot system (the scion, pronounced *sai* • uhn), a graft junction is formed, with vascular connections connecting the two systems into a single organism (Thomas & Frank, 2019). Hormones, tissue regeneration, and molecular pathways regulating vascular development are important to this process (Melnyk, 2017; Nanda & Melnyk, 2018). Often, the rootstock and scion are genetically distinct, combining two genotypes into a single chimera if no genetic incompatibility arises (Thomas *et al.*, 2022). When genetically distinct root and shoot systems are grafted together (a heterograft), they can be compared to different grafted rootstock and scion genotypes, the same genotype grafted to itself (a homograft), or an ungrafted plant (own-rooted) (Frank & Chitwood, 2016). Any difference in scion or rootstock traits relative to a different combination of grafted genotypes can be used to infer the genetic basis of reciprocal communication between root and shoot systems. Graft-induced signaling between genotypes has been used extensively during domestication, breeding, and agricultural improvement of crops (Williams *et al.*, 2021).

Grafting can be performed across the flowering plants (Reeves *et al.*, 2022). Especially in long-lived, woody perennials, grafting can be necessary for cultivation and even domestication itself (Warschefsky *et al.*, 2016). In perennial species, grafting has been used to modulate scion architecture through dwarfing, to alter fruit bearing through precocity and productivity, to change fruit quality, and to confer pathogen resistance and abiotic stress tolerance (Warschefsky *et al.*,

bioRxiv preprint doi: https://doi.org/10.1101/2022.05.17.492371; this version posted May 17, 2022. The copyright holder for this preprint (which was not certified by peer review) is the author/funder, who has granted bioRxiv a license to display the preprint in perpetuity. It is made available under aCC-BY-NC 4.0 International license.

2016). Over 80% of vineyards grow grafted grapes, a process that became widespread in response to the phylloxera (*Daktulosphaira vitifoliae* Fitch) crisis, in which grafting to tolerant and/or resistant rootstocks derived from North American *Vitis* species allowed wine and table grape scions to grow in infested soils (Ollat *et al.*, 2016). Subsequently, grapevine rootstocks were recognized as not only conferring resistance to pathogens besides phylloxera (Cousins & Walker, 2002; Hwang *et al.*, 2010; Ferris *et al.*, 2012), but also salinity and drought tolerance (Zhang *et al.*, 2002; Serra *et al.*, 2014), as well as altering scion mineral composition (Walker *et al.*, 2004; Gautier *et al.*, 2018, 2020; Migicovsky *et al.*, 2019; Harris *et al.*, 2022) and the chemistry and maturation of berries (Ruhl, 1989; Walker *et al.*, 2000; Kodur, 2011; Cheng *et al.*, 2017). One of the most desirable properties that grapevine rootstocks can affect is Ravaz (or harvest) index: the ratio of yield to pruning weight (or, 1-year-old cuttings weighed the following dormant season at pruning). A high Ravaz index is desirable to maximize yield and minimize vine management. However, in some cases, a Ravaz index may be too high, indicating that the vine is overcropped and often resulting in reduced fruit quality and reduced vine size (Bravdo *et al.*, 1984). Grapevine rootstocks modulate both components of Ravaz index, yield and vigor (McCarthy & Cirami, 1990; Ezzahouani & Williams, 1995; Jones *et al.*, 2009; Migicovsky *et al.*, 2021). Water and nutrient uptake are two of the principal means by which rootstocks affect reproductive and vegetative growth, consequently also influencing berry composition (Keller, 2020).

Although rootstocks can influence grapevine growth, yield, and berry qualities, the primary source of variation in these traits is the environment (Kidman *et al.*, 2014; Keller, 2020). In non-grafted plants, the root and shoot systems are in constant communication with each other. In particular, the root and shoot systems must communicate to enable hydraulic conductivity, the movement of water from the roots through the vasculature of plants to the leaves and other aerial parts where it is transpired (evaporated) or guttated (exuded). Through water uptake and vasculature, both environment and rootstocks converge on an often overlooked component of plant growth in perennial crops: secondary growth. The effects of the environment on secondary growth in woody perennials can be so strong that, using methods from dendrochronology, the widths of tree rings can be used to infer water availability and the length of the growing season. In angiosperms, the vascular cambium divides during the growing season to create xylem vessels and fibers (Rathgeber *et al.*, 2016). The daughter cells enlarge, thicken secondary walls, and eventually undergo cell death to form the empty lumen that transports water from the root to shoot systems. Grapevines and other vines and lianas have ring porous wood and produce wider vessels early in the season and narrow vessels later (Pratt, 1974; Ewers *et al.*, 1990; Wheeler & LaPasha, 1994). Grapevine annual ring width is environmentally responsive. In 14 year old *Vitis vinifera* L. cv. Merlot grafted to 140 Ruggeri (Munitz *et al.*, 2018) and 12 year old *V. vinifera* L. cv. ‘Cabernet sauvignon’ grafted to 140 Ruggeri (Netzer *et al.*, 2019), annual ring width, vessel diameter, and hydraulic conductivity all increase with applied water, most strongly at the beginning of the growing season when cambial activity is strongest (Berstein & Fahn, 1960).

Grapevine wood anatomy is also affected by grafting. Five year old *V. vinifera* L. cv. Piedirosso vines grafted to 420A have more numerous, narrower vessels in late wood compared to ungrafted counterparts, conferring safer water transport under drought conditions (De Micco *et*

bioRxiv preprint doi: https://doi.org/10.1101/2022.05.17.492371; this version posted May 17, 2022. The copyright holder for this preprint (which was not certified by peer review) is the author/funder, who has granted bioRxiv a license to display the preprint in perpetuity. It is made available under aCC-BY-NC 4.0 International license.

al., 2018). A comparison of wood anatomy between seven year old *V. vinifera* L. cv. Cabernet Sauvignon vines grafted to Riparia Gloire, 420A, and 1103 Paulsen found that a narrow rootstock stem size restricted hydraulic conductivity and affected physiological performance compared to a smoother graft junction with less discrepancy in rootstock and scion stem diameters (Shtein *et al.*, 2017). The extent and success of grafting may also play a role in the effect of rootstock on scion. For example, in a recent study of the effects of alignment of scion and rootstock, vine growth was significantly impacted in the nursery and the first year of establishment when there was partial alignment. However, in years 2 and 3, these differences disappeared (Marín *et al.*, 2022).

Here, using X-ray Computed Tomography (CT) to examine ring widths in 30 year old Chardonnay and Cabernet Sauvignon scion wood grafted to 15 different rootstocks from a California vineyard, we measured the effects of rootstocks on secondary growth. Within the size ranges of each scion, rootstock additively modulates scion trunk radius across a continuous range differing by up to 143% in width. Modeling ring width as a function of ring number, we find that scion modulates the widths of the first rings, whereas rootstock modulates decay, cumulatively affecting secondary growth throughout the lifetime of the vine. Traits collected early and late during the lifetime of the vineyard show correlations with scion trunk radius, including juice pH and Ravaz index, reflecting effects on vegetative growth. Consistent with previous work, scion trunk radius is also correlated with physiological performance, affecting photosynthetic assimilation, transpiration rate, and stomatal conductance. Our results show that the cumulative effects of grapevine rootstocks on viticultural traits act consistently over decades by altering physiological performance through scion wood anatomy.

Materials and Methods

Vineyard history, management, and design

A complete history of the vineyard sampled in this study is available in Migicovsky *et al.* (2021), reprinted here for convenience. In 1991 rootstocks were planted near Lodi in San Joaquin County, California, before scionwood was whip-grafted to the planted rootstock in 1992. The scion cutting was a cane (1 year old wood) when it was grafted. The soil type was a Tokay fine sandy loam soil. Vines were grafted to the following rootstocks: Freedom, Ramsey, 1103 Paulsen, 775 Paulsen, 110 Richter, 3309 Couderc, Kober 5BB, SO4, Teleki 5C, 101-14 Mgt, 039-16, 140 Ruggeri, Schwarzman, 420 A, and K51-32. The parental *Vitis* species for each rootstock are presented in **Table 1** (Hardie & Cirami, 1988; Riaz *et al.*, 2019). The two scion varieties were Chardonnay (selection FPS 04) and Cabernet Sauvignon (selection FPS 07). Rows were oriented east-west with vine spacing of 2.13 m by 3.05 m. The trellis system was a bilateral cordon with fixed foliage wires and the vines were cordon trained and spur pruned. The experimental design was a randomized complete block design, split between Chardonnay and Cabernet Sauvignon. There were four replications per treatment (rootstock). There were eight or nine vines per plot, except for Kober 5BB and SO4, which had four or five vines each, to fit all treatments in the block.

Trait collection

bioRxiv preprint doi: https://doi.org/10.1101/2022.05.17.492371; this version posted May 17, 2022. The copyright holder for this preprint (which was not certified by peer review) is the author/funder, who has granted bioRxiv a license to display the preprint in perpetuity. It is made available under aCC-BY-NC 4.0 International license.

Historical data across 8 traits and all 15 rootstocks were collected for 5 years, from 1995 to 1999, and described in Migicovsky *et al.* (2021). These traits were: soluble solids content, titratable acidity, pH, berry weight, cluster number, yield, pruning weight, and Razav index (a measurement of crop load calculated by dividing yield by pruning weight from the following dormant season). Contemporary data for all 15 rootstocks were also collected for 4 years, from 2017 to 2020, for the 8 traits included in the historical data set. Berry measurements were not calculated for 5BB Kober and SO4 in 2017 only, due to sample mislabelling at the time. In addition to the 8 traits from the historical data, numerous additional traits were collected for one or more years in the contemporary data set, including petiole nutrition measurements, cordon length, and yeast assimilable nitrogen (YAN). For a full summary of the number of measured samples for each trait included in analysis, for each scion, for each year, see **Supporting Information Table S1**.

In addition to these datasets, sampling took place at the vineyard for physiological measurements in 2018 and 2019. This sampling was performed using only 3 of the rootstocks, for each scion: Teleki 5C, Freedom, and 1103 Paulsen. In 2018, sampling was performed once a week for 8 weeks from June 19th, 2018 to August 6th, 2018. In 2019, sampling was performed once a week for 7 weeks from June 17th, 2019 to July 29th, 2019. For each rootstock x scion combination, 3 vines were sampled, and for each vine, 2 leaves were measured. Measurements were subsequently averaged across leaves from a particular vine. The same 2 leaves were measured for both physiological traits and leaf temperature.

Physiological traits were measured using a portable photosynthesis system (LI-6800, LICOR Biosciences, Lincoln, NE, USA) on clear sky days. Flow (600 µmol s^{-1}), H_20 (RH_air 50%), C_20 (CO2_r 400 µmol mol^{-1}), temperature (Tleaf 33 °C), and light (1800 µmol m^{-2} s^{-1}) were kept constant throughout sampling periods. Three measurements were taken: stomatal conductance (GSW, mol m□² s□¹), photosynthetic CO2 rate (A, µmol m□² s□¹), and transpiration rate (E, mol m□² s□¹). Fully expanded, sunlight leaves were measured, and each leaf was from a different shoot on the vine and selected to represent the canopy as a whole. Measurements were taken midday (approximately 10:30 am – 2:30 pm). Leaf temperature measurements were taken either immediately before or after the physiological measurements using an infrared thermometer (Extech 42515), scanning the same leaves measured for physiological traits.

X-ray Computed Tomography and ring measurement

All trunk samples were collected on March 2, 2021 using a chainsaw. Trunk sections were roughly 20 cm long and taken 15-20 cm below the cordon wire (101.6 cm height) at the head of the vine, normally just below cordon split. Given that 1 year old scionwood was grafted in 1992 and cuttings of it were taken in 2021, the physiological age of the trunk samples was 30 years old, although the vineyard itself was only 29 years old. Samples were placed in polyethylene bags, sealed, and shipped to Michigan State University. CT images were taken from the middle of the vine samples. The total image height was approximately 95 cm. Images were scanned at 75 kV and 450 µamps in continuous mode with 2880 projections and 2 frames averaged on a

bioRxiv preprint doi: https://doi.org/10.1101/2022.05.17.492371; this version posted May 17, 2022. The copyright holder for this preprint (which was not certified by peer review) is the author/funder, who has granted bioRxiv a license to display the preprint in perpetuity. It is made available under aCC-BY-NC 4.0 International license.

North Star Imaging X3000. The focal spot size was 33.75 microns and the detector was set to 12.5 frames per second. Scan time was 8 minutes. Scans were reconstructed using the efX-CT software from North Star Imaging (Rogers, MN). Final voxel resolution was 63.9 µm and pixel resolution was 63.9 µm by 63.9 µm (0.00639 cm by 0.00639 cm). From each 3D CT image, three individual slices were taken for analysis. One slice was from the top of the image, one was from the middle of the image, and the last was from the bottom of the image. All slices were aligned to be taken perpendicular to the vine samples. In ImageJ (Abràmoff *et al.*, 2004). A thin line was drawn from the center of the pith to the bark avoiding eccentric growth and crossing rings as perpendicular as possible. Landmarks were placed according to **Figure 1A**. Euclidean distance converting from pixels to centimeters was used to calculate ring widths. Models of ring width as a function of ring number were fitted with the three slices per each vine. Ring width measurements across the 3 slices for each vine were averaged for trait correlation analysis.

Data analysis

Data analysis was performed in Python (v. 3.7.3) using Jupyter notebooks (v. 1.0.0) (Kluyver *et al.*, 2016). Numpy (v. 1.19.4) (Harris *et al.*, 2020) and Pandas (v. 1.3.5) (McKinney, 2011) were used to work with arrays and dataframes and Matplotlib (v. 3.1.0) (Hunter, 2007) and Seaborn (v. 0.11.2) (Waskom, 2021) were used for visualization. The negative exponential model $ring\ width\ = A\ + B * e^{-k * ring\ number}$ was fit using the curve_fit() function from Scipy (v. 1.7.3) (Virtanen *et al.*, 2020). The Statsmodels module (v. 0.13.2) (Seabold & Perktold, 2010) was used to perform ordinary least squares (OLS) and analysis of variance (ANOVA) modeling as well as for using the Benjamini-Hochberg (BH) procedure for multiple-test correction. The .corr() function in Pandas was used to calculate Spearman's rank correlation coefficient. For correlations between scion trunk radius and physiological traits, the repeated measures correlation coefficient (r_{rm}) was calculated using the Pingouin module (v. 0.5.1) (Vallat, 2018). The repeated measures correlation coefficient (Bakdash & Marusich, 2017) fits an overall correlation coefficient on a population of repeated measures. In our case the repeated measures are physiological measurements on scions with three different rootstocks (Teleki 5C, Freedom, and 1103 Paulsen) on 15 different dates across 2018 and 2019. All code and data to reproduce the results and visualizations in this manuscript, with comments and narrative, can be found in a Jupyter notebook https://github.com/DanChitwood/grapevine_rings/blob/main/grapevine_ring_analysis_v2.ipynb.

Results

Variation in scion trunk radius arises from cumulative effects of rootstocks on ring width

Scion trunk radius varies most strongly by scion, but within scion, rootstock exerts a strong additive effect (**Figure 1B-C**). For the model $scion\ trunk\ radius \sim scion * rootstock$, scion explains 46.53% of variation ($p = 3.50 \times 10^{-15}$) in scion trunk radius and rootstock 16.57% ($p = 0.0057$), while the interaction effect only 2.42% ($p = 0.980$) (**Table 2**). Scion shifts the range of scion trunk radii conferred by rootstocks in an additive fashion. Within Chardonnay, the median scion trunk radius arising from the rootstock conferring the widest radius (775 Paulsen, 4.05 cm)

bioRxiv preprint doi: https://doi.org/10.1101/2022.05.17.492371; this version posted May 17, 2022. The copyright holder for this preprint (which was not certified by peer review) is the author/funder, who has granted bioRxiv a license to display the preprint in perpetuity. It is made available under aCC-BY-NC 4.0 International license.

is 143% wider than the rootstock conferring the narrowest radius (Schwarzmann, 2.84 cm) (**Figure 1B**). The same rootstocks define the range of scion trunk radii within Cabernet Sauvignon and closely follow the order of that in Chardonnay, with the rootstock conferring the widest radius (775 Paulsen, 4.94 cm) 129% wider than that conferring the narrowest (Schwarzmann, 3.83 cm) (**Figure 1C**).

Tree ring widths can be modeled as a function of ring number using a negative exponential model (Fritts *et al.*, 1969). We applied the model $ring\ width\ = A\ + B * e^{-k*ring\ number}$ to measure how scion and rootstock modulate ring width across the scion trunk. Comparing the overall model to models fitted with +/- 1.5 standard deviations from the mean values for A, B, and k shows how each of these variables acts (**Figure 2A**). A transposes ring width, including the asymptote, up and down across all rings, B affects the widths of the first rings but not the asymptote of the later rings, and k affects the decay, how rapidly the ring width approaches the asymptote. For all rings, modeled width was higher in Cabernet Sauvignon than Chardonnay (**Figure 2B-C**), consistent with scion trunk radii (**Figure 1**). If models of ring width are calculated for each rootstock for each scion, differences in decay are observed by rootstock (**Figure 2D-E**). For example, one of the rootstocks conferring a wider scion trunk radius (1103 Paulsen, dark green in **Figure 2D-E**) maintains higher ring widths, whereas one of the rootstocks conferring a narrower scion trunk radius (Teleki 5C, dark pink in **Figure 2D-E**) rapidly drops in ring width value after the first couple rings. Additionally Cabernet Sauvignon has higher ring widths in the first couple rings compared to Chardonnay, but both scions fall to a similar asymptote around 0.2 cm in later rings. To quantify these trends, we calculated modeled A, B, and k values for each vine (**Figure 2F-H**) and analyzed how they vary across scion and rootstock variables using the model $\boldsymbol{trait \sim scion * rootstock}$ (**Table 2**)**.** No terms were significant for A, which is the translation of the curve along the y axis, but $rootstock$ was almost significant with p = 0.0565 and explained 22.21% of the variation (**Table 2**). $scion$ explains 13.67% of variation in B, the spread of the early rings, and is highly significant (p = 0.000068) while $rootstock$ explains more variability at 19.01% but was much less significant (p = 0.0593). For k, the decay, only $rootstock$ was significant (p = 0.0298) explaining 22.68% of the variation. We conclude that scion modulates the widths of the first rings, as evidenced by being highly significant for modulating modeled B values. Rootstock, contrastingly, modulates ring widths more consistently throughout the trunk and across the lifetime of the vine by modulating the decay, k (**Table 2**).

Ravaz (harvest) index and juice pH are robustly correlated with scion ring and trunk width

To determine traits most correlated with ring features and if there are specific ring features that correlate with specific traits, we correlated all traits with all ring features. The ring features were modeled A, B, and k values (**Figure 2F-H**), early and late ring widths 1 to 8, outer ring widths, cambium, and total width (or, scion trunk radius). Only rings 1 to 8 were measured individually because after these, boundaries between rings and early and late wood became indistinguishable. As described in Materials and Methods and detailed in **Supporting Information Table S1**, some traits were collected only during 1995-1999, others 2017-2020, and some for both periods. To understand general trends in the data, we visualized the

bioRxiv preprint doi: https://doi.org/10.1101/2022.05.17.492371; this version posted May 17, 2022. The copyright holder for this preprint (which was not certified by peer review) is the author/funder, who has granted bioRxiv a license to display the preprint in perpetuity. It is made available under aCC-BY-NC 4.0 International license.

distribution of correlation coefficients for each trait, for each scion, across the years the trait was measured with scion trunk radius, as an overall summary (**Figure 3A**). Median Spearman's rank correlation coefficient values between traits and scion trunk radius range from around -0.4 to 0.4. Some traits have similar correlation coefficient values between the two scions, while others are contrasting. For example, whereas pruning weight is strongly positively correlated with scion trunk radius in both scions, juice pH is similarly positively correlated in Chardonnay, but more neutral in Cabernet Sauvignon. Yield divided by pruning weight (also known as harvest, or specifically in grapevines as Ravaz, index) is strongly negatively correlated in both Chardonnay and Cabernet Sauvignon. In contrast, petiole tissue Mg and Ca traits were strongly negatively correlated with scion trunk radius in Chardonnay and more neutral in Cabernet Sauvignon (**Figure 3A**).

Multiple test adjustment on 5,786 correlations between each ring feature with trait values for each scion and for each year resulted in 26 significant correlations with $p \leq 0.05$ (**Figure 3B**).

Our strategy in correlating each trait against each ring feature was to agnostically determine if the traits measured in years corresponding to rings (or preceding years, given the patterning of grapevine organs the year before they emerge) (Khanduja & Balasubrahmanyam, 1972; Srinivasan & Mullins, 1976; Guilpart *et al.*, 2014; Chitwood *et al.*, 2021) showed associations with each other. We did not detect any specific associations of rings with traits measured for the years they were patterned. Further, rather than building chronologies and correcting for age-related growth trends as is typically done in dendrochronology studies, we leverage the fact that all vines are the same age, allowing the widths for each ring across vines to be compared with each other. Significant correlations tended to include Chardonnay and traits measured in 1995-1999; however, this does not mean that Cabernet Sauvignon or traits measured in 2017-2020 are necessarily more weakly correlated with ring features, as these factor levels have relatively more missing data points as a result of both missing ring data (**Figure 1**) and trait data (**Supporting Information Table S1**). The missing ring data was generally a result of vines which had become scion-rooted over time and could therefore not be accurately sampled for rootstock-effects. Of the 26 significant correlations, 11 include Ravaz index and 8 juice pH (**Figure 3B**). Harvest index tended to be negatively correlated with ring and trunk widths while juice pH was positively correlated. There were no strong patterns of specific ring features correlating with traits except that there were no significant correlations with cambium width and that there were more correlations with late wood (12) compared to early wood (5). The correlation between Ravaz index and scion trunk radius was consistently negative across 1995-1999 in both Chardonnay and Cabernet Sauvignon, although the correlations were stronger and driven by variability in vines with smaller scion trunk radii in Chardonnay (**Figure 4A**). The negative correlation in Ravaz index with ring features is driven by strong positive correlations between pruning weight and ring width in both scions (**Figure 3A**). Vines with larger ring widths tended to produce more vegetative growth (higher pruning weight) while the impact on reproductive growth (yield) was weak. As a result, Ravaz index had a high negative correlation with scion trunk radius, indicating that vines with larger trunks had lower ratios of yield/pruning weight. Similar to Ravaz index, the positive correlation between juice pH and scion trunk radius is maintained in Chardonnay across 1995-1999 but is not significant for Cabernet Sauvignon (**Figure 4B**).

bioRxiv preprint doi: https://doi.org/10.1101/2022.05.17.492371; this version posted May 17, 2022. The copyright holder for this preprint (which was not certified by peer review) is the author/funder, who has granted bioRxiv a license to display the preprint in perpetuity. It is made available under aCC-BY-NC 4.0 International license.

Impact of scion trunk radius on vine physiology

To determine the physiological implications of rootstock choice, assimilation rate (A), transpiration rate (E), stomatal conductance (gsw), and leaf temperature were measured for 15 dates during the 2018-2019 growing seasons. To better synchronously measure time-intensive physiological traits with replication, three rootstocks were chosen that happen to span low to high scion trunk radius values: from low to high, Teleki 5C, Freedom, and 1103 Paulsen (**Figure 1B-C**). The repeated measures correlation coefficient (r_{rm}), which fits an overall correlation coefficient value to a population of multiple measurements (Bakdash & Marusich, 2017), was used (**Figure 5**). Measurements on the three rootstocks, measured for each scion of each of the 15 dates, were used as repeated measures to calculate an overall correlation coefficient between each physiological trait and scion trunk radius. Repeated measure correlation coefficients for assimilation rate, transpiration rate, and stomatal conductance with scion trunk radius, for both Chardonnay and Cabernet Sauvignon, were positive, ranging between 0.28 and 0.37, and highly significant. The same correlations for leaf temperature, measured using an infrared temperature gun on the same leaves from which physiological traits were taken, were near 0 and not significant. For the rootstocks spanning scion trunk radius values that were measured, we conclude that vines with wider trunks are more photosynthetically active, both transpiring and assimilating more (**Figure 5**).

Discussion

Within the scion trunk radius ranges of Chardonnay and Cabernet Sauvignon, rootstocks modulate size in an additive, continuous fashion up to 143% (**Figure 1B-C**). These results build upon and support previous observations comparing seven year old Cabernet Sauvignon grafted onto 1103 Paulsen, 420A, and Riparia Gloire (Shtein *et al.*, 2017). Although our study does not include Riparia Gloire, which had an unusually small trunk diameter (and which was proposed as a mechanism by which hydraulic conductance and physiological performance are limited), we confirm that Cabernet Sauvignon grafted onto 1103 Paulsen has a wider scion trunk radius than 420A. Similarly, De Micco *et al*. (2018), in comparing five year old ungrafted Piedirosso to vines grafted to 420A, found that grafting limits hydraulic conductivity in desirable ways, increasing berry quality. Rather than a binary view of graft formation either inhibiting or permitting hydraulic conductance as a consequence of trunk diameter and wood anatomy, in comparing 15 rootstocks, we instead observe a continuous range of scion trunk radii. In using two scions, we also see that these effects are additive, layered on top of the larger scion effect, mostly preserving the ranking of scion trunk radii conferred by different rootstocks (**Figure 1**; **Table 2**).

Scion trunk radius is the summation of annual ring widths and by measuring the outcome of 30 years of growth, we are able to identify the mechanisms by which rootstocks alter wood anatomy (**Figure 2**). Using the model $ring\ width = A + B * e^{-k*ring\ number}$, scion most strongly modulates B, the spread of the first rings (**Figure 2A; Table 2**). Considering that scions were whip grafted to rootstocks in their first year of growth, scion effects are expected to dominate in

bioRxiv preprint doi: https://doi.org/10.1101/2022.05.17.492371; this version posted May 17, 2022. The copyright holder for this preprint (which was not certified by peer review) is the author/funder, who has granted bioRxiv a license to display the preprint in perpetuity. It is made available under aCC-BY-NC 4.0 International license.

the absence of any rootstock. Rootstock most strongly modulates the decay of ring width k thereafter, which can be interpreted as a consistent effect across all rings for the lifetime of the grafted vine. How rootstocks modulate annual ring width is illuminated by previous studies demonstrating how the environment does so. In grapevines and other lianas, rings arise from high cambial activity early in the growing season and less at the end, creating the alternating seasonal pattern of early and late wood (Berstein & Fahn, 1960; Pratt, 1974; Kozlowski, 1983; Ewers *et al.*, 1990; Wheeler & LaPasha, 1994). As shown previously by Munitz *et al.* (2018), ring width increases with water availability, especially in the early growing season (late deficit) when cambial activity is greatest. Hypotheses of rootstocks (Shtein *et al.*, 2017) and grafting (De Micco *et al.*, 2018) altering physiological performance by restricting hydraulic conductance are derived from extrapolating from these well-studied environmental effects of water availability in the early season coinciding with meristem activity and the development of wood anatomy.

The impact of environment and rootstocks on physiological performance are derived both from ring width and trunk diameter as well as parallel changes in vessel anatomy affecting overall hydraulic conductivity of the vine. Generally in vines vessel length and diameter are correlated with stem diameter (Ewers & Fisher, 1989; Jacobsen *et al.*, 2012, 2015) and grafting impacts vessel frequency and size in peach, cherry, and apple as well (Olmstead *et al.*, 2006; Gonçalves *et al.*, 2007; Tombesi *et al.*, 2009). Density of vessels is not affected by irrigation, but overall vessel diameter and diameter of large vessels increases with water availability, especially under late deficit in the early growing season (Munitz *et al.*, 2018; Netzer *et al.*, 2019). A previous study noted increases in the frequency of more narrow vessels in late wood in response to grafting (De Micco *et al.*, 2018). However, when considered with annual ring width and the distribution of vessel diameters, grafting reduces hydraulic conductivity (De Micco *et al.*, 2018) and rootstocks with larger trunk diameters increase it (Shtein *et al.*, 2017). Vessels are visible in our X-ray CT images and can be measured (**Figure 1**), but as the pixel resolution is limited to 63.9 µm, we are unable to measure narrow vessel diameters that constitute an important segment of vessels in the bimodal distribution of grapevine (Munitz *et al.*, 2018) and which grafting is reported to increase in frequency (De Micco *et al.*, 2018). The impacts of rootstocks on hydraulic connectivity can nonetheless be inferred from physiological performance, as photosynthetic assimilation rate, transpiration rate, and stomatal conductance all decrease when water status is impaired (Romero & Martinez-Cutillas, 2012). Across these three rootstocks, we observe highly significant correlations between physiological parameters known to be affected by hydraulic conductivity with scion trunk radius (**Figure 5**). Although the extent of alignment between rootstock and scion was not evaluated in this study, vines with complete alignment may have higher levels of transpiration than those with partial alignment, indicating that the success of grafting itself may also play a role in physiological differences. However, in previous work this did not correspond to hydraulic conductivity differences across the graft measured in three year old vines at the end of the study (Marín *et al.*, 2022).

Vegetative growth can indicate water availability (Tyree & Ewers, 1991; Munitz *et al.*, 2017), and from this perspective it is not surprising that some of the most correlated traits with rootstock-induced changes in scion trunk radii are related to growth (**Figures 3-5**). Indeed, a previous study of this vineyard suggested that the 1998 reduction in yield observed may be due to a dry

bioRxiv preprint doi: https://doi.org/10.1101/2022.05.17.492371; this version posted May 17, 2022. The copyright holder for this preprint (which was not certified by peer review) is the author/funder, who has granted bioRxiv a license to display the preprint in perpetuity. It is made available under aCC-BY-NC 4.0 International license.

1997 dormant season (Migicovsky *et al.*, 2021). The cumulative precipitation for 1997 was 2,533 inches. In comparison, precipitation for 1995, 1996, 1998, and 1999, ranged from 3,377 to 7,775 inches, indicating that there was substantially more rainfall during these years (Migicovsky *et al.*, 2021). The 1998 season is one of the same years where the correlation with Ravaz index, the ratio of yield to pruning weight, is weak for both Chardonnay and Cabernet Sauvignon (**Figure 4A**). However, overall, the correlations with Ravaz index are some of the strongest. As scion trunk radius increases in Chardonnay, Ravaz index decreases, driven mostly by year-to-year variation in vines with narrow trunk diameters from 1995 to 1999 (**Figure 4A**). The relationship is less strong for Cabernet Sauvignon. Similar to 1998, the correlation with the Ravaz index from 1996 is also poor. Both 1996 and 1998 were years previously reported to have low yields, and as a result, low Ravaz indexes. Although the reason for low yields in 1996 is unclear, among the 1995-1999 data, it was the year with the highest pruning weights, indicating a stronger investment in vegetative growth (Migicovsky *et al.*, 2021). Underlying the strongest correlations between Ravaz index and scion trunk radius observed in both scions are years of higher yields and lower pruning weights (1995, 1997, and 1999) (**Figure 3A**), thus indicating that in years that enable high reproductive growth, yields are lower in large scions. While there was a modestly positive correlation between yield and scion trunk radius in Cabernet Sauvignon, the correlation for Chardonnay was modestly negative which likely explains why the correlation between Ravaz index and scion trunk radius was higher for Chardonnay. Taken together, these findings indicate that generally vines with a larger trunk radius will have a lower Ravaz index as a result of having higher vegetative growth (pruning weight). This relationship is stronger in Chardonnay, which also generally had smaller vines (**Figure 1B**) as well as lower yields in comparison to Cabernet Sauvignon (Migicovsky *et al.*, 2021). A lower Ravaz index is not desirable for grape growers, because it leads to higher management costs relative to the increase in profit (or yield).

Similar to pruning weight, juice pH had a strong positive correlation with scion trunk radius, but only in Chardonnay, which was consistently observed across 1995 to 1999 (**Figures 3, 4**). Juice pH is potentially influenced by potassium uptake of rootstocks (Ruhl, 1989; Kodur, 2011), but we did not observe strong correlations between petiole potassium levels and scion trunk radius (**Figure 3A**). We mention correlations with juice pH because it is strongly positive and scion-specific, and it is consistent across years (**Figure 4B**), in addition to showing that effects on hydraulic conductivity and growth associated with ring width and trunk diameter can potentially affect berry quality through indirect mechanisms of water and nutrient uptake (Keller *et al.*, 2012; Mantilla *et al.*, 2018; Migicovsky *et al.*, 2019). We focus on the correlation of traits with scion trunk radius as a cumulative indicator of rootstock-mediated effects on scion annual ring widths, but in correlating with each ring feature, we note that there are only 5 significant correlations with early wood ring widths compared to 12 significant correlations with late wood ring widths (**Figure 3B**). De Micco *et al.* (2018) also note that grafting induces more, narrower vessels creating wider latewood rings compared to ungrafted vines. Although speculation, it might be that water availability in the early season environment corresponding with cambial activity mostly affects early wood ring width (Munitz *et al.*, 2017; Netzer *et al.*, 2019) whereas rootstocks act relatively more on latewood and narrower vessels (**Figure 3B**; (De Micco *et al.*,

bioRxiv preprint doi: https://doi.org/10.1101/2022.05.17.492371; this version posted May 17, 2022. The copyright holder for this preprint (which was not certified by peer review) is the author/funder, who has granted bioRxiv a license to display the preprint in perpetuity. It is made available under aCC-BY-NC 4.0 International license.

2018)), contributing to a consistent genetic, environmentally-independent mechanism of modulating wood anatomy.

Regardless of mechanism, our results show that rootstocks act consistently over decades to modulate growth and other scion traits. Although the significant correlations after multiple test adjustments are biased by small amounts of missing data (**Figure 3B**; **Supporting Information Table S1**), the strength, direction, and scion-specificity of the correlations are consistent for traits from the beginning (1995-1999) to the end (2017-2020) of the 30 year life of the vineyard we studied (**Figure 3A**). Vessels in *V. vinifera* are only active 1-3 years before inactivation and no vessels are active after 7 years (Pratt, 1974; Tibbetts & Ewers, 2000; Pratt & Jacobsen, 2018). From this perspective, the continuous range of scion trunk radii conferred by grapevine rootstocks (**Figure 1**) is a symptom and consequence of consistent modulation of wood anatomy across the years (**Figure 2**) that renews the hydraulic effects on rootstocks on viticultural traits (**Figures 3-4**) through physiological mechanisms (**Figure 5**). Just as used in dendrochronology to infer climatic conditions from secondary growth, annual rings can be used as a way to allow the vines themselves to report on genetic and environmental effects that are modulating their performance. The wide-ranging and continuous effects of rootstocks on scion wood anatomy are a powerful way that grape growers can precisely modulate the vegetative growth versus yield, and indirectly berry and resulting wine quality, by altering hydraulic conductivity consistently over years, with important implications for the use of rootstocks in all woody perennial species.

Conflicts of Interest

JLK, DRH, LJ, RKS, and PC were employed by E&J Gallo Winery. The remaining authors declare that the research was conducted in the absence of any commercial or financial relationship that could be construed as a potential conflict of interest.

Funding Statement

ALD and DHC were supported by the USDA National Institute of Food and Agriculture, and by Michigan State University AgBioResearch. ALD is supported by a USDA National Institute of Food and Agriculture McIntire-Stennis Capacity grant. ZM, JFS, MK, PC, and DHC were supported by the National Science Foundation Plant Genome Research Program #1546869.

Acknowledgements

We gratefully acknowledge all the individuals involved in maintaining the vineyard evaluated for this study, in particular Ernie and Jeff Dosio (Pacific Agrilands Inc., Modesto, CA). We also thank Alex Freeman (Michigan State University) for early contributions to data analysis.

Author Contribution

bioRxiv preprint doi: https://doi.org/10.1101/2022.05.17.492371; this version posted May 17, 2022. The copyright holder for this preprint (which was not certified by peer review) is the author/funder, who has granted bioRxiv a license to display the preprint in perpetuity. It is made available under aCC-BY-NC 4.0 International license.

ZM, JFS, JLH, DRH, LMJ, MK, RKS, and PC collected vineyard trait data and/or prepared wood for analysis. MYG and JM collected and prepared X-ray CT images. DHC measured ring widths. TA, ARA, JDD, BMG, IK, MRM, ELM, AWS, ALD, SS, and DHC analyzed data. ZM and DHC coordinated research, data analysis, and manuscript writing. DHC wrote a first draft of the manuscript which all authors read, commented on, and edited.

Data Availability

X-ray CT cross-sections with landmarks are deposited on Dryad: http://dx.doi.org/10.5061/dryad.gqnk98sqf. All data and code to reproduce results are posted on the Github repository https://github.com/DanChitwood/grapevine_rings.

Supporting Information Table S1: Numbers of measured samples for each trait, for each scion, for each year.

Table 1: Rootstock parentage

Rootstock	Parentage
775 Paulsen	*V. berlandieri* Rességuier 2 × *V. rupestris* du Lot
1103 Paulsen	*V. berlandieri* Rességuier 2 × *V. rupestris* du Lot
3309 Couderc	*V. riparia x V. rupestris*
110 Richter	*V. berlandieri* Boutin B × *V. rupestris* du Lot
Kober 5BB	*V. berlandieri* Rességuier 2 × *V. riparia* Gloire de Montpellier
039-16	*V. vinifera* Almeria x *V. rotundifolia* Male No. 1
SO4	*V. berlandieri* Rességuier 2 × *V. riparia* Gloire de Montpellier
Freedom	Fresno 1613- 59 × Dog Ridge 5
Ramsey	*Vitis* x *champinii*
140 Ruggeri	*V. berlandieri* Boutin B × *V. rupestris* du Lot
420A	*V. berlandieri* x *V. riparia*
101-14 MGT	*V. riparia x V. rupestris*
K51-32	*V.* x *champinii, V. riparia*
Teleki 5C	*V. berlandieri* Rességuier 2 × *V. riparia* Gloire de Montpellier
Schwarzmann	Unknown *V. rupestris* × *V. riparia* Gloire de Montpellier

bioRxiv preprint doi: https://doi.org/10.1101/2022.05.17.492371; this version posted May 17, 2022. The copyright holder for this preprint (which was not certified by peer review) is the author/funder, who has granted bioRxiv a license to display the preprint in perpetuity. It is made available under aCC-BY-NC 4.0 International license.

Table 2: For traits scion trunk radius and A, B, and k values from the model $ring\ width = A + B * e^{-k*ring\ number}$, the percent variation explained and p values for each factor in the model $trait \sim scion * rootstock$

	Scion		Rootstock		Scion x Rootstock	
Trait	Percent variation	p value	Percent variation	p value	Percent variation	p value
Scion trunk radius	46.53%	3.50×10^{-15}	16.57%	0.0057	2.42%	0.980
A	1.78%	0.160	22.21%	0.0565	10.35%	0.632
B	13.67%	0.000068	19.01%	0.0593	10.64%	0.470
k	0.33%	0.527	22.68%	0.0298	16.86%	0.139

bioRxiv preprint doi: https://doi.org/10.1101/2022.05.17.492371; this version posted May 17, 2022. The copyright holder for this preprint (which was not certified by peer review) is the author/funder, who has granted bioRxiv a license to display the preprint in perpetuity. It is made available under aCC-BY-NC 4.0 International license.

Figures

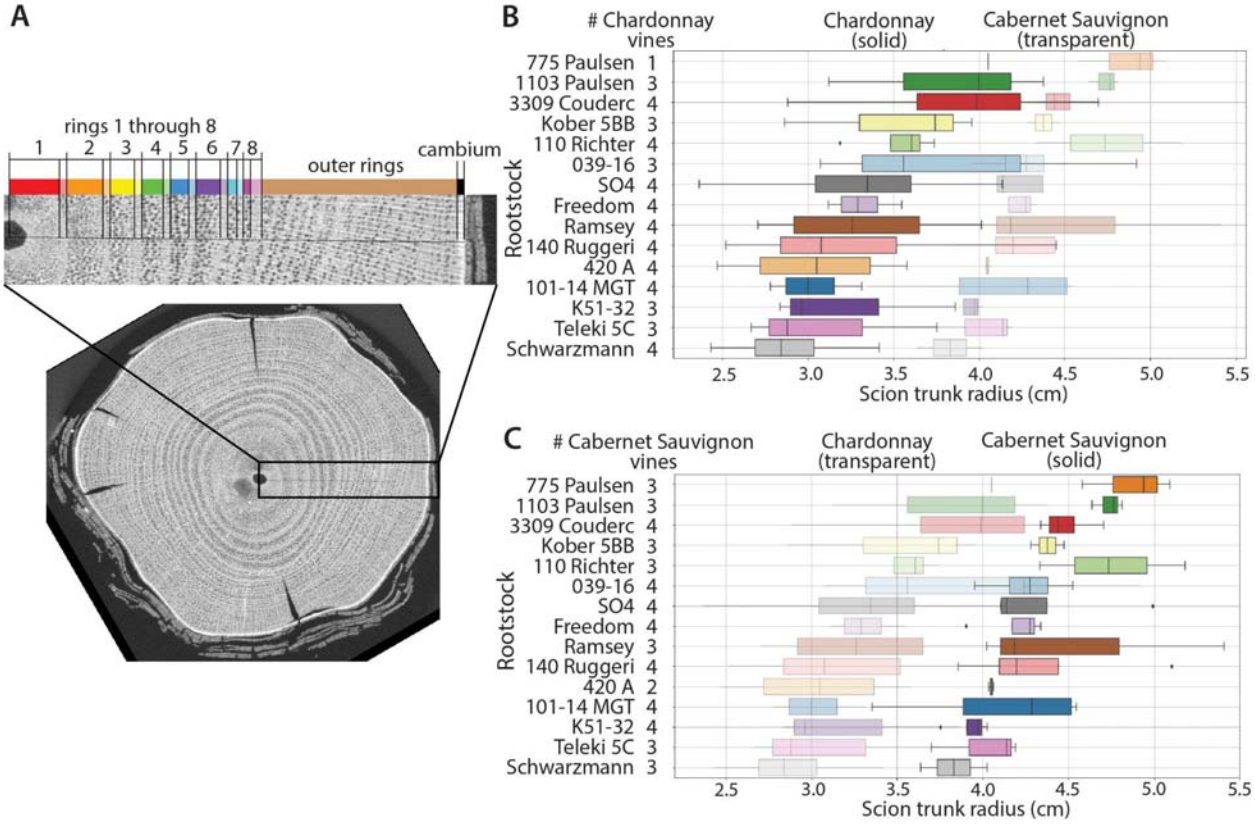

Figure 1: Grapevine rings and scion trunk radii. A) X-ray CT cross-section through a grapevine trunk. Along a line from the center of the pith to bark, landmarks are placed indicating early (darker shade color) and late (lighter shade color) wood, the remaining outer rings, and cambium. **B-C)** Boxplots showing distributions of scion trunk radii (cm) in **B)** Chardonnay (solid) relative to Cabernet Sauvignon (transparent) and number of Chardonnay vines measured and **C)** Cabernet Sauvignon (solid) relative to Chardonnay (transparent) and number of Cabernet Sauvignon vines measured.

bioRxiv preprint doi: https://doi.org/10.1101/2022.05.17.492371; this version posted May 17, 2022. The copyright holder for this preprint (which was not certified by peer review) is the author/funder, who has granted bioRxiv a license to display the preprint in perpetuity. It is made available under aCC-BY-NC 4.0 International license.

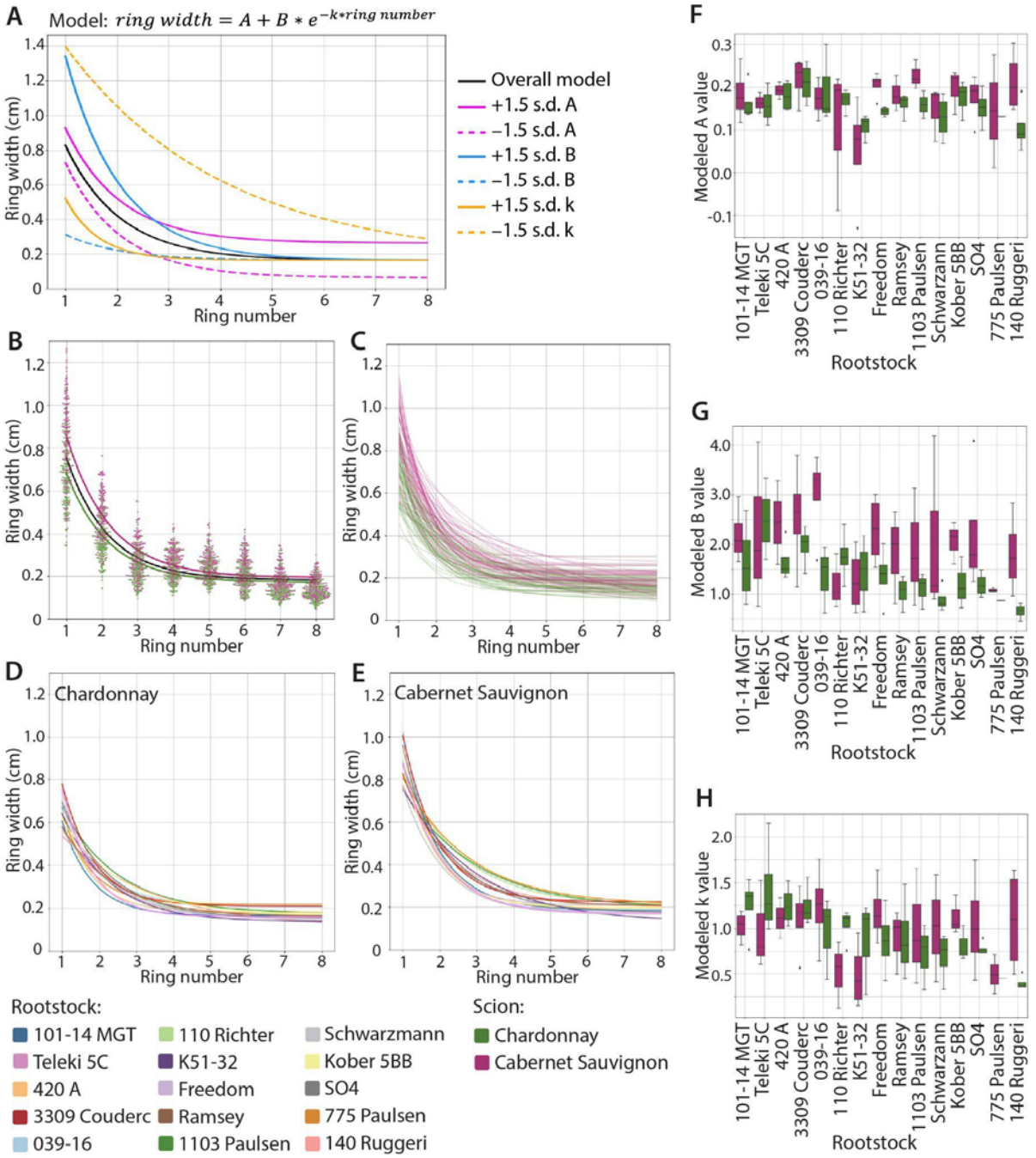

Figure 2: Models of ring width. A) For the negative exponential model $ring\ width = A + B * e^{-k*ring\ number}$, the overall model fitted to all the data (black solid line) and models fitted with values +1.5 standard deviations (solid lines) and -1.5 standard deviations (dashed lines) for A (magenta lines), B (blue lines), and k (orange lines). **B)** A swarmplot of all measured ring widths for Chardonnay (green) and Cabernet Sauvignon (purple) with an overall model (black) and models for each scion, **C)** models for each vine measured colored by scion, **D)** models for each rootstock for Chardonnay scions, and **E)** models for each rootstock for Cabernet Sauvignon scions. **F-H)** Boxplots of model values by rootstock and by scion for **F)** A, **G)** B, and **H)** k.

bioRxiv preprint doi: https://doi.org/10.1101/2022.05.17.492371; this version posted May 17, 2022. The copyright holder for this preprint (which was not certified by peer review) is the author/funder, who has granted bioRxiv a license to display the preprint in perpetuity. It is made available under aCC-BY-NC 4.0 International license.

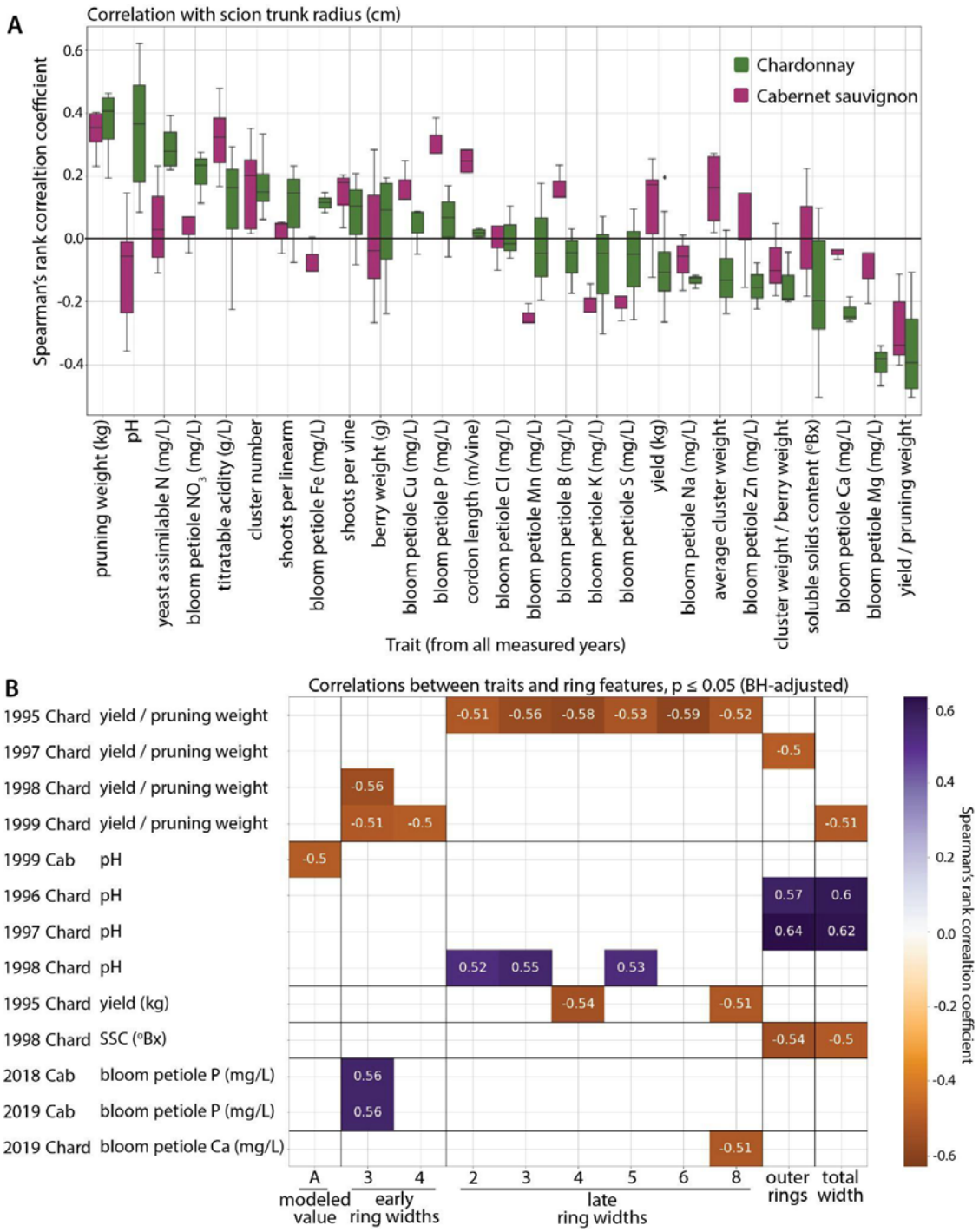

Figure 3: Correlations between ring features and traits. A) Boxplot showing distributions of Spearman's rank correlation coefficient values for correlation between indicated traits for Chardonnay (green) and Cabernet Sauvignon (purple) and scion trunk radius (cm). **B)** 26 traits that remain significant at $p < 0.05$ after Benjamini-Hochberg multiple test correction. The year, scion, and trait as well as ring features (modeled values, early ring widths, late ring widths, outer ring width, or total width) are indicated. Negative (burnt orange) to positive (violet) correlation coefficient values are indicated by scale and also provided by text for each correlation.

bioRxiv preprint doi: https://doi.org/10.1101/2022.05.17.492371; this version posted May 17, 2022. The copyright holder for this preprint (which was not certified by peer review) is the author/funder, who has granted bioRxiv a license to display the preprint in perpetuity. It is made available under aCC-BY-NC 4.0 International license.

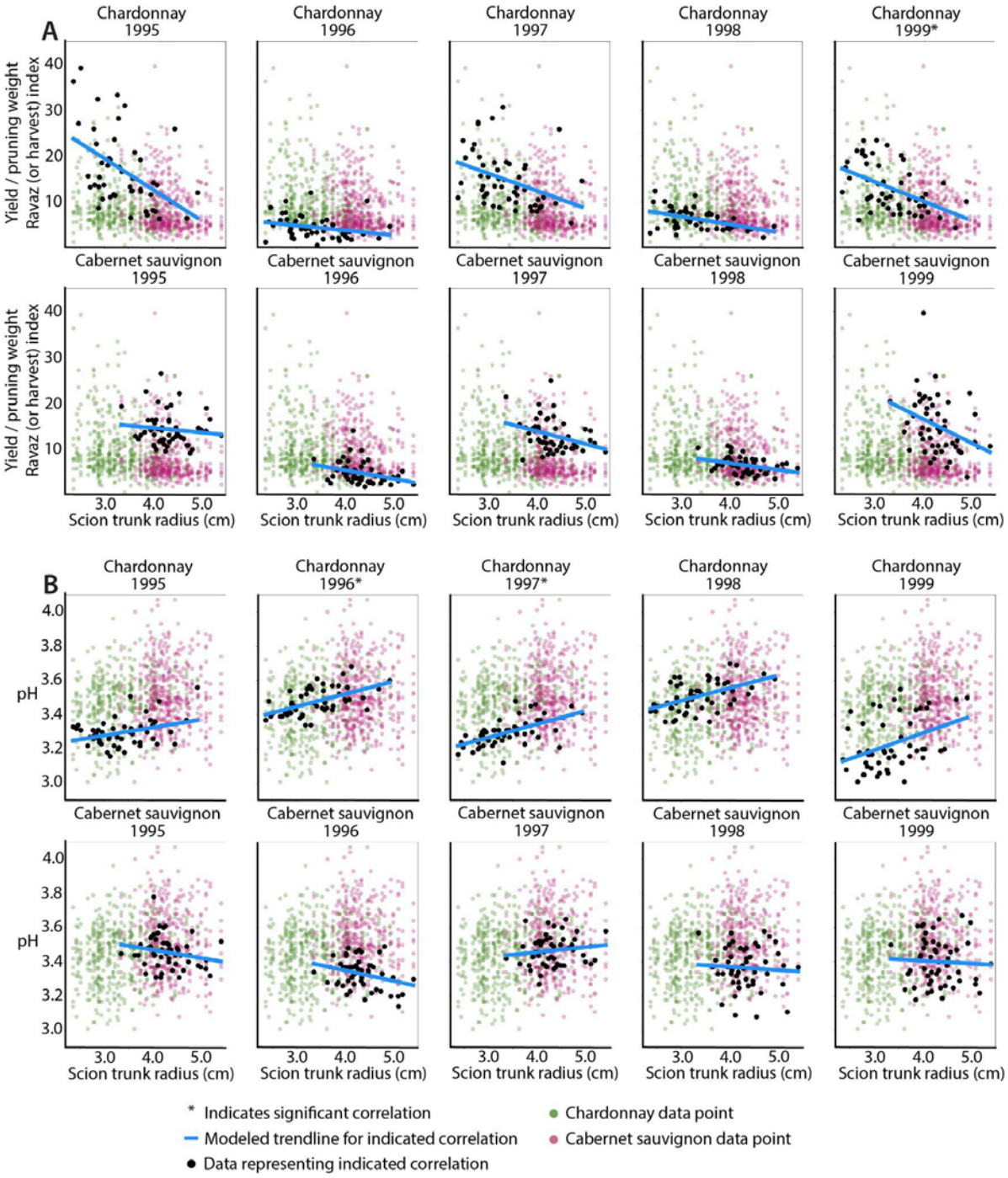

Figure 4: Correlations by year for harvest index and pH with scion trunk radius. Asterisks indicate significant correlations (as indicated in Figure 3B), based on multiple testing correction. For correlations between **A)** yield divided by pruning weight (harvest, or Ravaz, index) and **B)** juice pH correlations with scion trunk radius (cm) for data from each scion and indicated year (black data points) and a modeled trendline (blue) are superimposed over all data for the trait (Chardonnay, green; Cabernet Sauvignon, purple) across the years shown.

bioRxiv preprint doi: https://doi.org/10.1101/2022.05.17.492371; this version posted May 17, 2022. The copyright holder for this preprint (which was not certified by peer review) is the author/funder, who has granted bioRxiv a license to display the preprint in perpetuity. It is made available under aCC-BY-NC 4.0 International license.

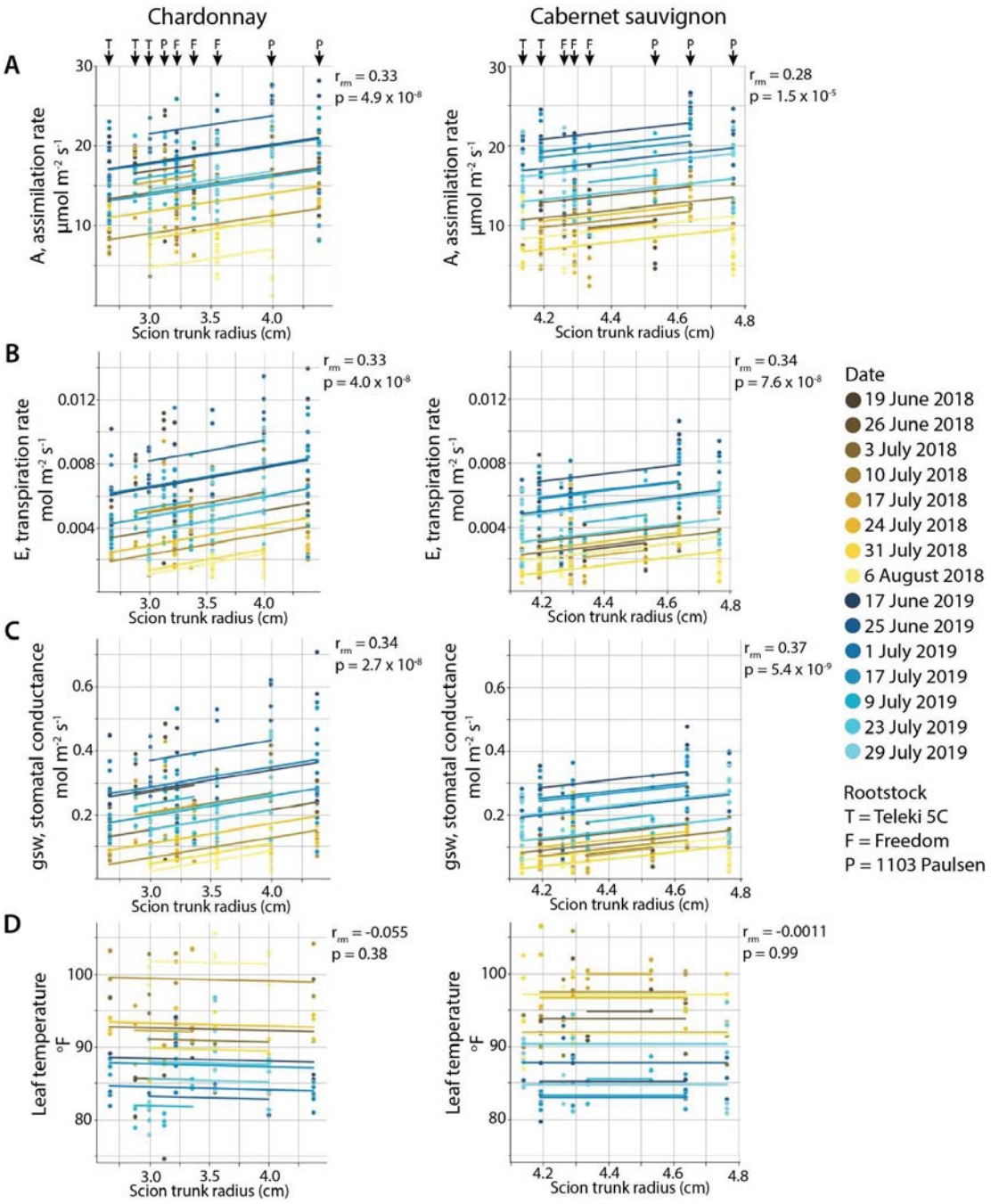

Figure 5: Repeated measures correlation between physiological traits and scion trunk radius for three rootstocks. Repeated measure correlation coefficient (r_{rm}) and p value are shown for the overall fitted correlation between **A)** A, assimilation rate (µmol $m^{-2}s^{-1}$), **B)** E, transpiration rate (mol $m^{-2}s^{-1}$), **C)** gsw, stomatal conductance (mol $m^{-2}s^{-1}$), and **D)** leaf temperature (^{o}F) with scion trunk radius (cm) across 3 rootstocks measured on 15 dates across two years. The scions and rootstocks (T = Teleki 5C, F = Freedom, and P = 1103 Paulsen) are indicated in the top panels and dates are indicated as shown by color, yellow shades for 2018 and blue for 2019.

bioRxiv preprint doi: https://doi.org/10.1101/2022.05.17.492371; this version posted May 17, 2022. The copyright holder for this preprint (which was not certified by peer review) is the author/funder, who has granted bioRxiv a license to display the preprint in perpetuity. It is made available under aCC-BY-NC 4.0 International license.

References

Abràmoff MD, Magalhães PJ, Ram SJ. **2004**. Image processing with ImageJ. *Biophotonics international* **11**: 36–42.

Bakdash JZ, Marusich LR. **2017**. Repeated measures correlation. *Frontiers in psychology* 8: 456.

Berstein Z, Fahn A. **1960**. The Effect of Annual and Bi-annual Pruning on the Seasonal Changes in Xylem Formation in the Grapevine: With five Figures in the Text. *Annals of Botany* **24**: 159–171.

Bravdo B, Hepner Y, Loinger C, Cohen S, Tabacman H. **1984**. Effect of crop level on growth, yield and wine quality of a high yielding Carignane vineyard. *American Journal of Enology and Viticulture* **35**: 247–252.

Cheng J, Wei L, Mei J, Wu J. **2017**. Effect of rootstock on phenolic compounds and antioxidant properties in berries of grape (Vitis vinifera L.) cv. 'Red Alexandria'. *Scientia Horticulturae* **217**: 137–144.

Chitwood DH, Mullins J, Migicovsky Z, Frank M, VanBuren R, Londo JP. **2021**. Vein-to-blade ratio is an allometric indicator of leaf size and plasticity. *American Journal of Botany* **108**: 571–579.

Cousins P, Walker M. **2002**. Genetics of resistance to Meloidogyne incognita in crosses of grape rootstocks. *Theoretical and Applied Genetics* **105**: 802–807.

De Micco V, Zalloni E, Battipaglia G, Erbaggio A, Scognamiglio P, Caputo R, Cirillo C. **2018**. Rootstock effect on tree-ring traits in grapevine under a climate change scenario. *IAWA journal* **39**: 145–155.

Ewers FW, Fisher JB. **1989**. Variation in vessel length and diameter in stems of six tropical and subtropical lianas. *American Journal of Botany* **76**: 1452–1459.

Ewers FW, Fisher JB, Chiu S-T. **1990**. A survey of vessel dimensions in stems of tropical lianas and other growth forms. *Oecologia* **84**: 544–552.

Ezzahouani A, Williams LE. **1995**. The influence of rootstock on leaf water potential, yield, and berry composition of Ruby Seedless grapevines. *American Journal of Enology and Viticulture* **46**: 559–563.

Ferris H, Zheng L, Walker M. **2012**. Resistance of grape rootstocks to plant-parasitic nematodes. *Journal of nematology* **44**: 377.

Frank MH, Chitwood DH. **2016**. Plant chimeras: The good, the bad, and the 'Bizzaria'. *Plant Development* **419**: 41–53.

Fritts HC, Mosimann JE, Bottorff CP. **1969**. A revised computer program for standardizing tree-ring series.

Gaut BS, Miller AJ, Seymour DK. **2019**. Living with Two Genomes: Grafting and Its Implications for Plant Genome-to-Genome Interactions, Phenotypic Variation, and Evolution. *Annual Review of Genetics* **53**.

Gautier A, Cookson SJ, Hevin C, Vivin P, Lauvergeat V, Mollier A. **2018**. Phosphorus acquisition efficiency and phosphorus remobilization mediate genotype-specific differences in shoot phosphorus content in grapevine. *Tree physiology* **38**: 1742–1751.

Gautier A, Cookson SJ, Lagalle L, Ollat N, Marguerit E. **2020**. Influence of the three main genetic backgrounds of grapevine rootstocks on petiolar nutrient concentrations of the scion, with a focus on phosphorus. *OENO One* **54**: 1–13.

Gonçalves B, Correia CM, Silva AP, Bacelar EA, Santos A, Ferreira H, Moutinho-Pereira JM. **2007**. Variation in xylem structure and function in roots and stems of scion–rootstock combinations of sweet cherry tree (Prunus avium L.). *Trees* **21**: 121–130.

Guilpart N, Metay A, Gary C. **2014**. Grapevine bud fertility and number of berries per bunch are determined by water and nitrogen stress around flowering in the previous year. *European*

bioRxiv preprint doi: https://doi.org/10.1101/2022.05.17.492371; this version posted May 17, 2022. The copyright holder for this preprint (which was not certified by peer review) is the author/funder, who has granted bioRxiv a license to display the preprint in perpetuity. It is made available under aCC-BY-NC 4.0 International license.

Journal of Agronomy **54**: 9–20.
Hardie W, Cirami R. **1988**. Grapevine rootstocks. In: Viticulture. Adelaide: Winetitles, 154–176.
Harris CR, Millman KJ, Van Der Walt SJ, Gommers R, Virtanen P, Cournapeau D, Wieser E, Taylor J, Berg S, Smith NJ. **2020**. Array programming with NumPy. *Nature* **585**: 357–362.
Harris ZN, Pratt JE, Bhakta N, Frawley E, Klein LL, Kwasniewski M, Migicovsky Z, Miller A. **2022**. Temporal and environmental factors interact with rootstock genotype to shape leaf elemental composition in grafted grapevines. : 2022.02.28.482393.
Hunter JD. **2007**. Matplotlib: A 2D graphics environment. *Computing in science & engineering* 9: 90–95.
Hwang C-F, Xu K, Hu R, Zhou R, Riaz S, Walker MA. **2010**. Cloning and characterization of XiR1, a locus responsible for dagger nematode resistance in grape. *Theoretical and Applied Genetics* **121**: 789–799.
Jacobsen AL, Pratt RB, Tobin MF, Hacke UG, Ewers FW. **2012**. A global analysis of xylem vessel length in woody plants. *American journal of botany* **99**: 1583–1591.
Jacobsen AL, Rodriguez-Zaccaro FD, Lee TF, Valdovinos J, Toschi HS, Martinez JA, Pratt RB. **2015**. Grapevine xylem development, architecture, and function. In: Functional and ecological xylem anatomy. Springer, 133–162.
Jones TH, Cullis BR, Clingeleffer PR, Rühl E. **2009**. Effects of novel hybrid and traditional rootstocks on vigour and yield components of Shiraz grapevines. *Australian Journal of Grape and Wine Research* **15**: 284–292.
Keller M. **2020**. Chapter 6: Developmental physiology. In: The Science of Grapevines. Academic Press, 199–277.
Keller M, Mills LJ, Harbertson JF. **2012**. Rootstock effects on deficit-irrigated winegrapes in a dry climate: Vigor, yield formation, and fruit ripening. *American Journal of Enology and Viticulture* **63**: 29–39.
Khanduja S, Balasubrahmanyam V. **1972**. Fruitfulness of grape vine buds. *Economic Botany* **26**: 280–294.
Kidman CM, Mantilla SO, Dry PR, McCarthy MG, Collins C. **2014**. Effect of water stress on the reproductive performance of Shiraz (Vitis vinifera L.) grafted to rootstocks. *American Journal of Enology and Viticulture* **65**: 96–108.
Kluyver T, Ragan-Kelley B, Pérez F, Granger BE, Bussonnier M, Frederic J, Kelley K, Hamrick JB, Grout J, Corlay S. **2016**. *Jupyter Notebooks-a publishing format for reproducible computational workflows.*
Kodur S. **2011**. Effects of juice pH and potassium on juice and wine quality, and regulation of potassium in grapevines through rootstocks (Vitis): a short review. *VITIS Journal of Grapevine Research* **50**: 1–6.
Kozlowski T. **1983**. *Water deficits and plant growth*. NY, USA: Academic Press.
Mantilla SMO, Collins C, Iland PG, Kidman CM, Ristic R, Boss PK, Jordans C, Bastian SE. **2018**. Shiraz (Vitis vinifera L.) berry and wine sensory profiles and composition are modulated by rootstocks. *American Journal of Enology and Viticulture* **69**: 32–44.
Marín D, Santesteban L g., Dayer S, Villa-Llop A, Abad F j., Gambetta G a., Torres-Ruiz J m., Torres N. **2022**. Connection matters: exploring the implications of scion–rootstock alignment in grafted grapevines. *Australian Journal of Grape and Wine Research* **n/a**.
McCarthy MG, Cirami RM. **1990**. The Effect of Rootstocks on the Performance of Chardonnay from a Nematode-Infested Barossa Valley Vineyard. *American Journal of Enology and Viticulture* **41**: 126–130.
McKinney W. **2011**. pandas: a foundational Python library for data analysis and statistics. *Python for high performance and scientific computing* **14**: 1–9.
Melnyk CW. **2017**. Plant grafting: insights into tissue regeneration. *Regeneration (Oxford, England)* 4: 3–14.
Migicovsky Z, Cousins P, Jordan LM, Myles S, Striegler RK, Verdegaal P, Chitwood DH.

bioRxiv preprint doi: https://doi.org/10.1101/2022.05.17.492371; this version posted May 17, 2022. The copyright holder for this preprint (which was not certified by peer review) is the author/funder, who has granted bioRxiv a license to display the preprint in perpetuity. It is made available under aCC-BY-NC 4.0 International license.

2021. Grapevine rootstocks affect growth-related scion phenotypes. *Plant Direct* 5: e00324.
Migicovsky Z, Harris ZN, Klein LL, Li M, McDermaid A, Chitwood DH, Fennell A, Kovacs LG, Kwasniewski M, Londo JP, *et al.*2019. Rootstock effects on scion phenotypes in a 'Chambourcin' experimental vineyard. *Horticulture Research* 6: 64.
Munitz S, Netzer Y, Schwartz A. **2017**. Sustained and regulated deficit irrigation of field-grown Merlot grapevines. *Australian Journal of Grape and Wine Research* **23**: 87–94.
Munitz S, Netzer Y, Shtein I, Schwartz A. **2018**. Water availability dynamics have long-term effects on mature stem structure in Vitis vinifera. *American Journal of Botany* **105**: 1443–1452.
Nanda AK, Melnyk CW. **2018**. The role of plant hormones during grafting. *Journal of Plant Research* **131**: 49–58.
Netzer Y, Munitz S, Shtein I, Schwartz A. **2019**. Structural memory in grapevines: early season water availability affects late season drought stress severity. *European Journal of Agronomy* **105**: 96–103.
Ollat N, Bordenave L, Tandonnet JP, Boursiquot JM, Marguerit E. **2016**. Grapevine rootstocks: origins and perspectives. *Acta Horticulturae*: 11–22.
Olmstead MA, Lang NS, Ewers FW, Owens SA. **2006**. Xylem vessel anatomy of sweet cherries grafted onto dwarfing and nondwarfing rootstocks. *Journal of the American Society for Horticultural Science* **131**: 577–585.
Pratt C. **1974**. Vegetative anatomy of cultivated grapes--a review. *American Journal of Enology and Viticulture* **25**: 131–150.
Pratt RB, Jacobsen AL. **2018**. Identifying which conduits are moving water in woody plants: a new HRCT-based method. *Tree Physiology* **38**: 1200–1212.
Rathgeber CB, Cuny HE, Fonti P. **2016**. Biological basis of tree-ring formation: a crash course. *Frontiers in Plant Science* 7: 734.
Reeves G, Tripathi A, Singh P, Jones MR, Nanda AK, Musseau C, Craze M, Bowden S, Walker JF, Bentley AR. **2022**. Monocotyledonous plants graft at the embryonic root–shoot interface. *Nature* **602**: 280–286.
Riaz S, Pap D, Uretsky J, Laucou V, Boursiquot J-M, Kocsis L, Andrew Walker M. **2019**. Genetic diversity and parentage analysis of grape rootstocks. *Theoretical and Applied Genetics*.
Romero P, Martinez-Cutillas A. **2012**. The effects of partial root-zone irrigation and regulated deficit irrigation on the vegetative and reproductive development of field-grown Monastrell grapevines. *Irrigation Science* **30**: 377–396.
Ruhl E. **1989**. Uptake and distribution of potassium by grapevine rootstocks and its implication for grape juice pH of scion varieties. *Australian Journal of Experimental Agriculture* **29**: 707–712.
Seabold S, Perktold J. **2010**. Statsmodels: Econometric and statistical modeling with python. In: Austin, TX, 61.
Serra I, Strever A, Myburgh PA, Deloire A. **2014**. Review: the interaction between rootstocks and cultivars (Vitis vinifera L.) to enhance drought tolerance in grapevine. *Australian Journal of Grape and Wine Research* **20**: 1–14.
Shtein I, Hayat Y, Munitz S, Harcavi E, Akerman M, Drori E, Schwartz A, Netzer Y. **2017**. From structural constraints to hydraulic function in three Vitis rootstocks. *Trees* **31**: 851–861.
Srinivasan C, Mullins M. **1976**. Reproductive anatomy of the grape-vine (Vitis vinifera L.): Origin and development of the anlage and its derivatives. *Annals of Botany* **40**: 1079–1084.
Thomas HR, Frank MH. **2019**. Connecting the pieces: uncovering the molecular basis for long-distance communication through plant grafting. *New Phytologist* **223**: 582–589.
Thomas H, Van den Broeck L, Spurney R, Sozzani R, Frank M. **2022**. Gene regulatory networks for compatible versus incompatible grafts identify a role for SlWOX4 during junction formation. *The Plant Cell* **34**: 535–556.
Tibbetts TJ, Ewers FW. **2000**. Root pressure and specific conductivity in temperate lianas: exotic Celastrus orbiculatus (Celastraceae) vs. native Vitis riparia (Vitaceae). *American Journal*

bioRxiv preprint doi: https://doi.org/10.1101/2022.05.17.492371; this version posted May 17, 2022. The copyright holder for this preprint (which was not certified by peer review) is the author/funder, who has granted bioRxiv a license to display the preprint in perpetuity. It is made available under aCC-BY-NC 4.0 International license.

731 *of Botany* **87**: 1272–1278.
732 **Tombesi S, Johnson RS, Day KR, DeJong TM**. **2009**. Relationships between xylem vessel
733 characteristics, calculated axial hydraulic conductance and size-controlling capacity of peach
734 rootstocks. *Annals of Botany* **105**: 327–331.
735 **Tyree MT, Ewers FW**. **1991**. The hydraulic architecture of trees and other woody plants. *New*
736 *Phytologist* **119**: 345–360.
737 **Vallat R**. **2018**. Pingouin: statistics in Python. *J. Open Source Softw.* 3: 1026.
738 **Virtanen P, Gommers R, Oliphant TE, Haberland M, Reddy T, Cournapeau D, Burovski E,**
739 **Peterson P, Weckesser W, Bright J**. **2020**. SciPy 1.0: fundamental algorithms for scientific
740 computing in Python. *Nature methods* **17**: 261–272.
741 **Walker RR, Blackmore DH, Clingeleffer, R P, Correll RL**. **2004**. Rootstock effects on salt
742 tolerance of irrigated field-grown grapevines (Vitis vinifera L. cv. Sultana) 2. Ion concentrations
743 in leaves and juice. *Australian Journal of Grape and Wine Research* **10**: 90–99.
744 **Walker RR, Read PE, Blackmore DH**. **2000**. Rootstock and salinity effects on rates of berry
745 maturation, ion accumulation and colour development in Shiraz grapes. *Australian Journal of*
746 *Grape and Wine Research* 6: 227–239.
747 **Warschefsky EJ, Klein LL, Frank MH, Chitwood DH, Londo JP, von Wettberg EJ, Miller**
748 **AJ**. **2016**. Rootstocks: Diversity, Domestication, and Impacts on Shoot Phenotypes. *Trends*
749 *Plant Sci* **21**: 418–37.
750 **Waskom ML**. **2021**. Seaborn: statistical data visualization. *Journal of Open Source Software* 6:
751 3021.
752 **Wheeler E, LaPasha C**. **1994**. Woods of the Vitaceae—fossil and modern. *Review of*
753 *Palaeobotany and Palynology* **80**: 175–207.
754 **Williams B, Ahsan MU, Frank MH**. **2021**. Getting to the root of grafting-induced traits. *Growth*
755 *and development 2021* **59**: 101988.
756 **Zhang X, Walker RR, Stevens RM, Prior LD**. **2002**. Yield-salinity relationships of different
757 grapevine (Vitis vinifera L.) scion-rootstock combinations. *Australian Journal of Grape and Wine*
758 *Research* 8: 150–156.

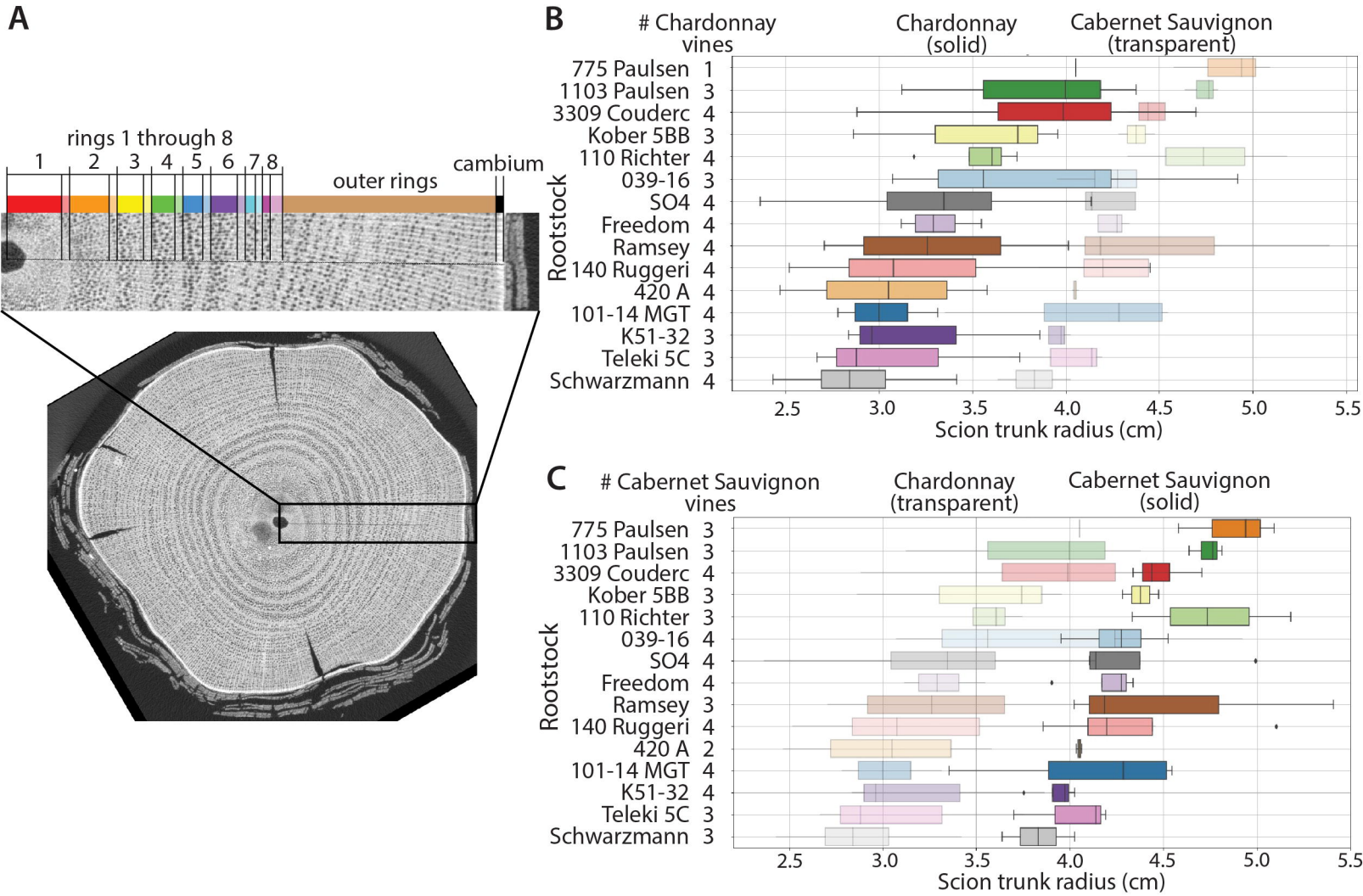
A
rings 1 through 8
1
2
3
4
5
6
7
8
outer rings
cambium
B
Chardonnay vines
Chardonnay (solid)
Cabernet Sauvignon (transparent)
Rootstock
775 Paulsen 1
1103 Paulsen 3
3309 Couderc 4
Kober 5BB 3
110 Richter 4
039-16 3
SO4 4
Freedom 4
Ramsey 4
140 Ruggeri 4
420 A 4
101-14 MGT 4
K51-32 3
Teleki 5C 3
Schwarzmann 4
2.5
3.0
3.5
4.0
4.5
5.0
5.5
Scion trunk radius (cm)
C
Cabernet Sauvignon vines
Chardonnay (transparent)
Cabernet Sauvignon (solid)
Rootstock
775 Paulsen 3
1103 Paulsen 3
3309 Couderc 4
Kober 5BB 3
110 Richter 3
039-16 4
SO4 4
Freedom 4
Ramsey 3
140 Ruggeri 4
420 A 2
101-14 MGT 4
K51-32 4
Teleki 5C 3
Schwarzmann 3
2.5
3.0
3.5
4.0
4.5
5.0
5.5
Scion trunk radius (cm)

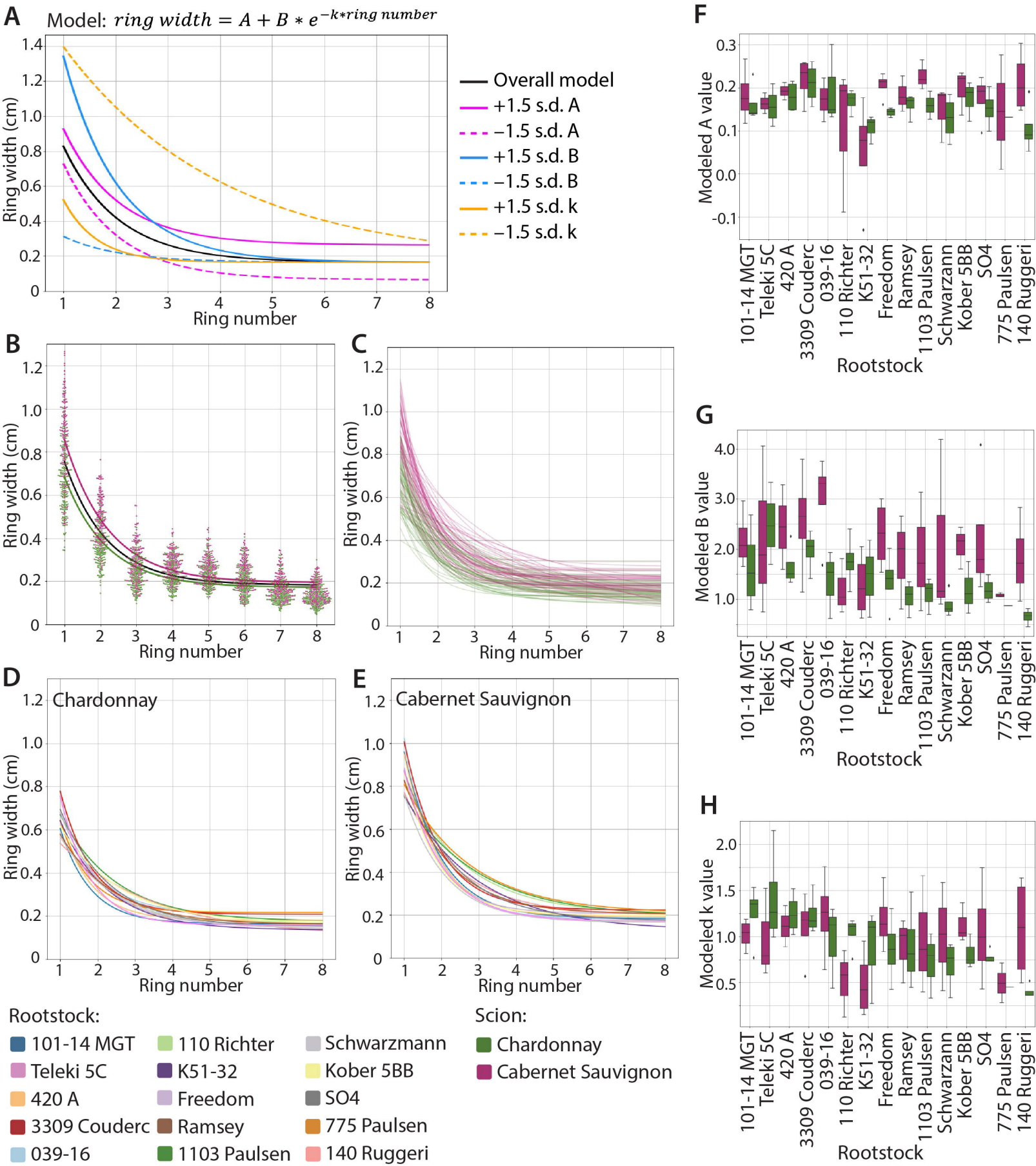
A
Model: $ring\ width = A + B * e^{-k*ring\ number}$
Ring width (cm)
Ring number
Overall model
+1.5 s.d. A
−1.5 s.d. A
+1.5 s.d. B
−1.5 s.d. B
+1.5 s.d. k
−1.5 s.d. k
B
C
D
Chardonnay
E
Cabernet Sauvignon
F
Modeled A value
G
Modeled B value
H
Modeled k value
Rootstock
101-14 MGT
Teleki 5C
420 A
3309 Couderc
039-16
110 Richter
K51-32
Freedom
Ramsey
1103 Paulsen
Schwarzmann
Kober 5BB
SO4
775 Paulsen
140 Ruggeri
Scion:
Chardonnay
Cabernet Sauvignon

Available under aCC BY-NC 4.0 International license.

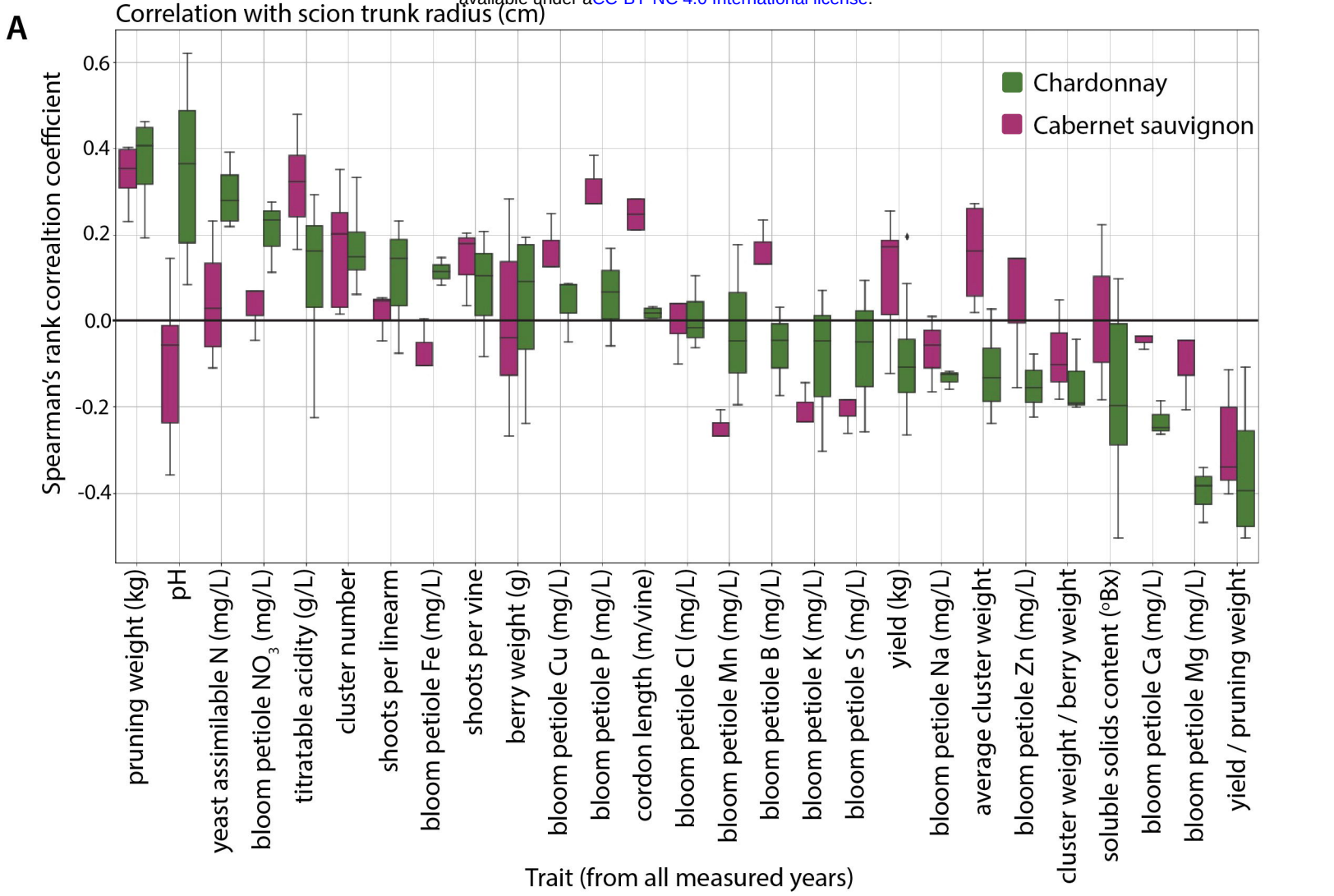

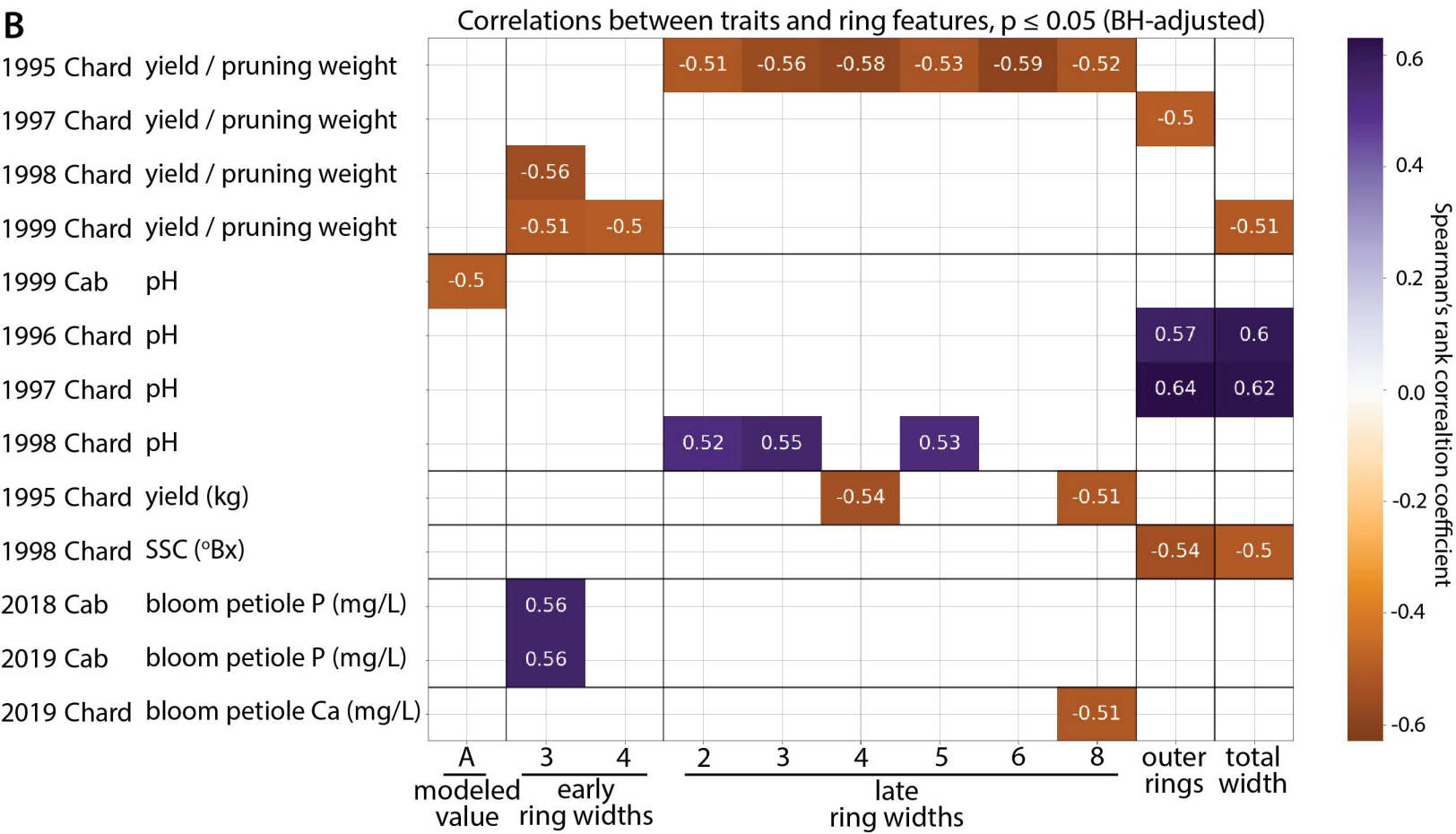

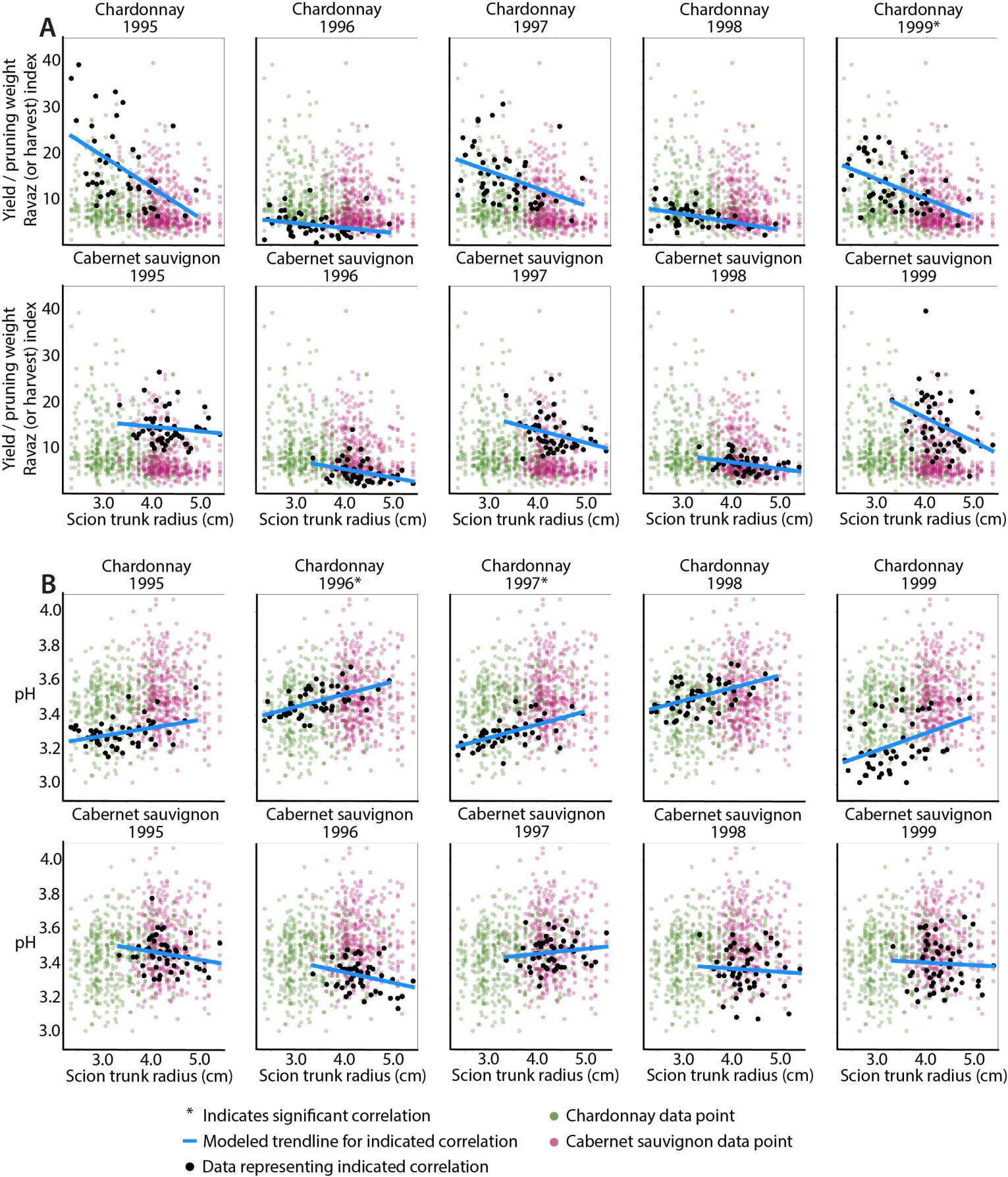
A
Chardonnay 1995
Chardonnay 1996
Chardonnay 1997
Chardonnay 1998
Chardonnay 1999*
Cabernet sauvignon 1995
Cabernet sauvignon 1996
Cabernet sauvignon 1997
Cabernet sauvignon 1998
Cabernet sauvignon 1999
Yield / pruning weight
Ravaz (or harvest) index
10
20
30
40
3.0
4.0
5.0
Scion trunk radius (cm)
B
Chardonnay 1995
Chardonnay 1996*
Chardonnay 1997*
Chardonnay 1998
Chardonnay 1999
Cabernet sauvignon 1995
Cabernet sauvignon 1996
Cabernet sauvignon 1997
Cabernet sauvignon 1998
Cabernet sauvignon 1999
pH
3.0
3.2
3.4
3.6
3.8
4.0
* Indicates significant correlation
Modeled trendline for indicated correlation
Data representing indicated correlation
Chardonnay data point
Cabernet sauvignon data point

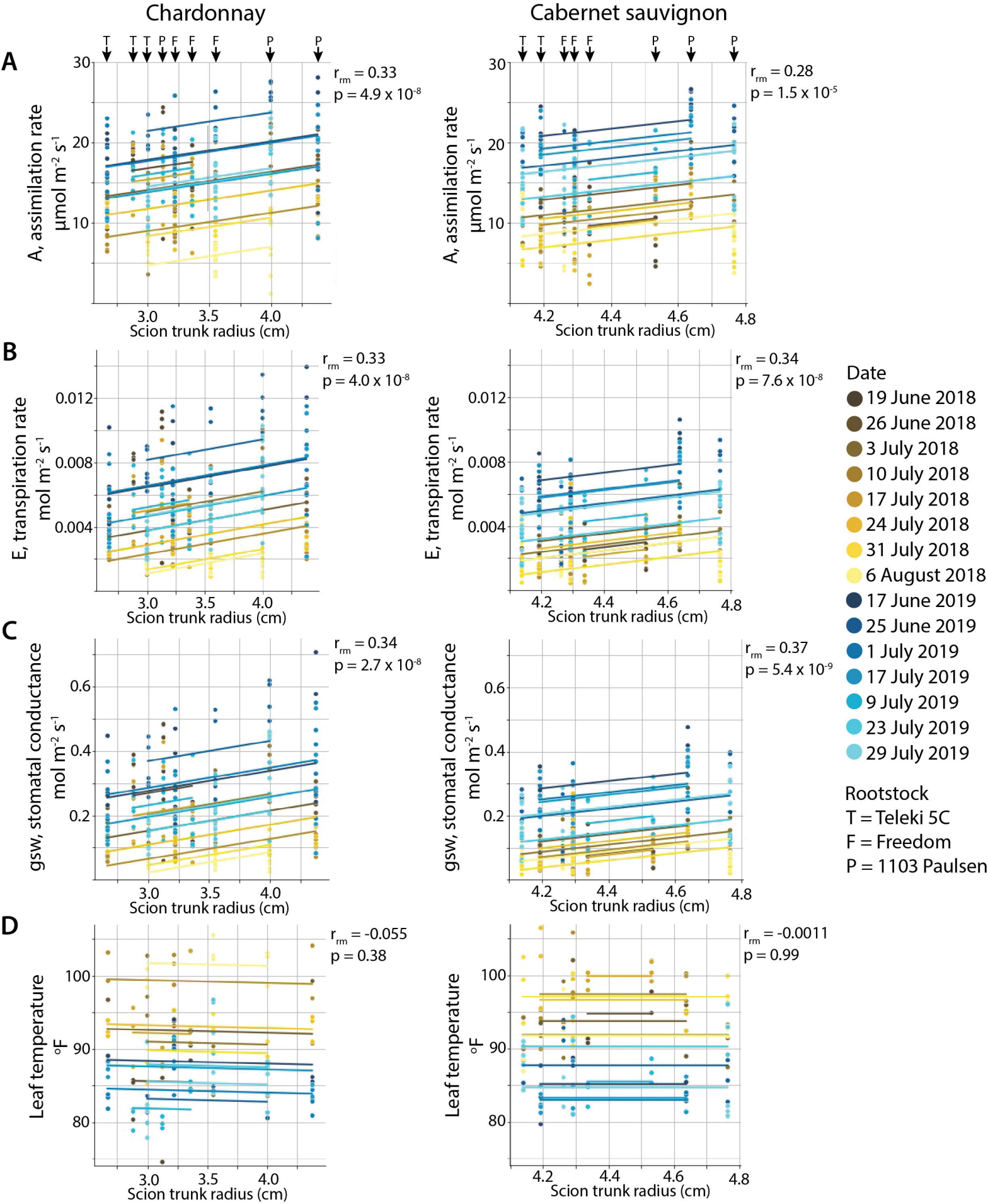
Chardonnay
Cabernet sauvignon
A
B
C
D
T T T P F F F P P
T T F F F P P P
A, assimilation rate
µmol m-2 s-1
E, transpiration rate
mol m-2 s-1
gsw, stomatal conductance
mol m-2 s-1
Leaf temperature
°F
Scion trunk radius (cm)
rrm = 0.33
p = 4.9 x 10-8
rrm = 0.28
p = 1.5 x 10-5
rrm = 0.33
p = 4.0 x 10-8
rrm = 0.34
p = 7.6 x 10-8
rrm = 0.34
p = 2.7 x 10-8
rrm = 0.37
p = 5.4 x 10-9
rrm = -0.055
p = 0.38
rrm = -0.0011
p = 0.99
Date
19 June 2018
26 June 2018
3 July 2018
10 July 2018
17 July 2018
24 July 2018
31 July 2018
6 August 2018
17 June 2019
25 June 2019
1 July 2019
17 July 2019
9 July 2019
23 July 2019
29 July 2019
Rootstock
T = Teleki 5C
F = Freedom
P = 1103 Paulsen